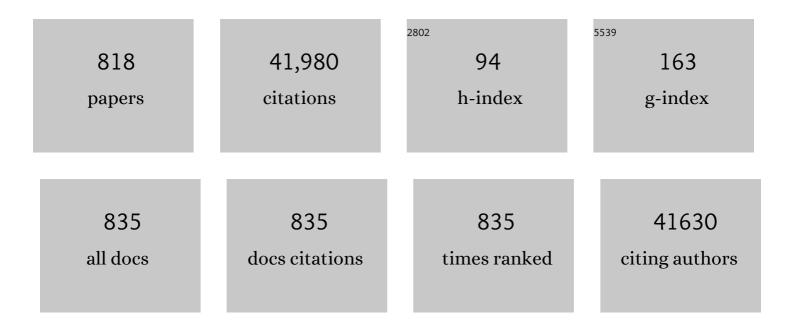
List of Publications by Year in descending order

Source: https://exaly.com/author-pdf/1274187/publications.pdf Version: 2024-02-01



#	Article	IF	CITATIONS
1	Mechanochemistry: opportunities for new and cleaner synthesis. Chemical Society Reviews, 2012, 41, 413-447.	38.1	2,281
2	Band alignment of rutile and anatase TiO2. Nature Materials, 2013, 12, 798-801.	27.5	1,924
3	Robust self-cleaning surfaces that function when exposed to either air or oil. Science, 2015, 347, 1132-1135.	12.6	1,494
4	Self-cleaning coatings. Journal of Materials Chemistry, 2005, 15, 1689.	6.7	855
5	Antimicrobial surfaces and their potential in reducing the role of the inanimate environment in the incidence of hospital-acquired infections. Journal of Materials Chemistry, 2009, 19, 3819.	6.7	458
6	Tuning the interlayer spacing of graphene laminate films for efficient pore utilization towards compact capacitive energy storage. Nature Energy, 2020, 5, 160-168.	39.5	381
7	Atmospheric Pressure Chemical Vapor Deposition of Tin Sulfides (SnS, Sn2S3, and SnS2) on Glass. Chemistry of Materials, 1999, 11, 1792-1799.	6.7	377
8	Intelligent Window Coatings:Â Atmospheric Pressure Chemical Vapor Deposition of Tungsten-Doped Vanadium Dioxide. Chemistry of Materials, 2004, 16, 744-749.	6.7	363
9	Alleviation of Dendrite Formation on Zinc Anodes via Electrolyte Additives. ACS Energy Letters, 2021, 6, 395-403.	17.4	340
10	Superhydrophobic polymer-coated copper-mesh; membranes for highly efficient oil–water separation. Journal of Materials Chemistry A, 2013, 1, 5943.	10.3	306
11	Titania and silver–titania composite films on glass—potent antimicrobial coatings. Journal of Materials Chemistry, 2007, 17, 95-104.	6.7	304
12	Evaluation of the BET Theory for the Characterization of Meso and Microporous MOFs. Small Methods, 2018, 2, 1800173.	8.6	288
13	n-Type doped transparent conducting binary oxides: an overview. Journal of Materials Chemistry C, 2016, 4, 6946-6961.	5.5	287
14	Characterisation of the photocatalyst Pilkington Activâ,,¢: a reference film photocatalyst?. Journal of Photochemistry and Photobiology A: Chemistry, 2003, 160, 213-224.	3.9	283
15	Preparation and Characterisation of Superâ€Hydrophobic Surfaces. Chemistry - A European Journal, 2010, 16, 3568-3588.	3.3	267
16	Ultrasensitive plano-concave optical microresonators for ultrasound sensing. Nature Photonics, 2017, 11, 714-719.	31.4	255
17	Bismuth oxyhalides: synthesis, structure and photoelectrochemical activity. Chemical Science, 2016, 7, 4832-4841.	7.4	252
18	The antimicrobial properties of light-activated polymers containing methylene blue and gold nanoparticles. Biomaterials, 2009, 30, 89-93.	11.4	231

#	Article	IF	CITATIONS
19	Self-Driven One-Step Oil Removal from Oil Spill on Water via Selective-Wettability Steel Mesh. ACS Applied Materials & Interfaces, 2014, 6, 19858-19865.	8.0	226
20	Aerosol-assisted delivery of precursors for chemical vapour deposition: expanding the scope of CVD for materials fabrication. Dalton Transactions, 2013, 42, 9406.	3.3	224
21	The Anti-Biofouling Properties of Superhydrophobic Surfaces are Short-Lived. ACS Nano, 2018, 12, 6050-6058.	14.6	222
22	Intelligent Multifunctional VO ₂ /SiO ₂ /TiO ₂ Coatings for Self-Cleaning, Energy-Saving Window Panels. Chemistry of Materials, 2016, 28, 1369-1376.	6.7	221
23	Intelligent window coatings: atmospheric pressure chemical vapour deposition of vanadium oxides. Journal of Materials Chemistry, 2002, 12, 2936-2939.	6.7	220
24	Novel TiO2 CVD films for semiconductor photocatalysis. Journal of Photochemistry and Photobiology A: Chemistry, 2002, 151, 171-179.	3.9	215
25	S, N oâ€Đoped Grapheneâ€Nickel Cobalt Sulfide Aerogel: Improved Energy Storage and Electrocatalytic Performance. Advanced Science, 2017, 4, 1600214.	11.2	204
26	Photo-induced enhanced Raman spectroscopy for universal ultra-trace detection of explosives, pollutants and biomolecules. Nature Communications, 2016, 7, 12189.	12.8	201
27	Rechargeable aqueous Zn-based energy storage devices. Joule, 2021, 5, 2845-2903.	24.0	201
28	Thick titanium dioxide films for semiconductor photocatalysis. Journal of Photochemistry and Photobiology A: Chemistry, 2003, 160, 185-194.	3.9	194
29	Insights on Flexible Zincâ€lon Batteries from Lab Research to Commercialization. Advanced Materials, 2021, 33, e2007548.	21.0	191
30	The role of surfaces in catheter-associated infections. Chemical Society Reviews, 2009, 38, 3435.	38.1	190
31	An investigation into bacterial attachment to an elastomeric superhydrophobic surface prepared via aerosol assisted deposition. Thin Solid Films, 2011, 519, 3722-3727.	1.8	181
32	Energy modelling studies of thermochromic glazing. Energy and Buildings, 2010, 42, 1666-1673.	6.7	175
33	The incorporation of noble metal nanoparticles into host matrix thin films: synthesis, characterisation and applications. Journal of Materials Chemistry, 2009, 19, 574-590.	6.7	173
34	Nanoparticles: their potential use in antibacterial photodynamic therapy. Photochemical and Photobiological Sciences, 2011, 10, 712-720.	2.9	173
35	Multi‣cale Investigations of δâ€Ni _{0.25} V ₂ O ₅ ·nH ₂ O Cathode Materials in Aqueous Zincâ€ion Batteries. Advanced Energy Materials, 2020, 10, 2000058.	19.5	173
36	Super-robust superhydrophobic concrete. Journal of Materials Chemistry A, 2017, 5, 14542-14550.	10.3	170

#	Article	IF	CITATIONS
37	Bulk magnetization of the heavy rare earth titanate pyrochlores - a series of model frustrated magnets. Journal of Physics Condensed Matter, 2000, 12, 483-495.	1.8	167
38	Superhydrophobic Photocatalytic Surfaces through Direct Incorporation of Titania Nanoparticles into a Polymer Matrix by Aerosol Assisted Chemical Vapor Deposition. Advanced Materials, 2012, 24, 3505-3508.	21.0	167
39	Investigation of a Branchlike MoO ₃ /Polypyrrole Hybrid with Enhanced Electrochemical Performance Used as an Electrode in Supercapacitors. ACS Applied Materials & Interfaces, 2014, 6, 1125-1130.	8.0	167
40	One pot synthesis of nickel foam supported self-assembly of NiWO ₄ and CoWO ₄ nanostructures that act as high performance electrochemical capacitor electrodes. Journal of Materials Chemistry A, 2015, 3, 14272-14278.	10.3	167
41	Large-scale fabrication of translucent and repairable superhydrophobic spray coatings with remarkable mechanical, chemical durability and UV resistance. Journal of Materials Chemistry A, 2017, 5, 10622-10631.	10.3	164
42	Intelligent Thermochromic Windows. Journal of Chemical Education, 2006, 83, 393.	2.3	162
43	Atmospheric Pressure Chemical Vapor Deposition of Crystalline Monoclinic WO3 and WO3-x Thin Films from Reaction of WCl6 with O-Containing Solvents and Their Photochromic and Electrochromic Properties. Chemistry of Materials, 2005, 17, 1583-1590.	6.7	161
44	Gas Sensing with Nano-Indium Oxides (In ₂ O ₃) Prepared via Continuous Hydrothermal Flow Synthesis. Langmuir, 2012, 28, 1879-1885.	3.5	160
45	Table Salt as a Template to Prepare Reusable Porous PVDF–MWCNT Foam for Separation of Immiscible Oils/Organic Solvents and Corrosive Aqueous Solutions. Advanced Functional Materials, 2017, 27, 1702926.	14.9	160
46	Palladium alloys used as electrocatalysts for the oxygen reduction reaction. Energy and Environmental Science, 2021, 14, 2639-2669.	30.8	158
47	Atmospheric pressure chemical vapour deposition of SnSe and SnSe2 thin films on glass. Thin Solid Films, 2008, 516, 4750-4757.	1.8	156
48	Nitrogen-doped TiO ₂ thin films: photocatalytic applications for healthcare environments. Dalton Transactions, 2011, 40, 1635-1640.	3.3	153
49	Creating superhydrophobic mild steel surfaces for water proofing and oil–water separation. Journal of Materials Chemistry A, 2014, 2, 11628-11634.	10.3	153
50	Aerosol Assisted Chemical Vapor Deposition Using Nanoparticle Precursors:Â A Route to Nanocomposite Thin Films. Journal of the American Chemical Society, 2006, 128, 1587-1597.	13.7	151
51	Titania and tungsten doped titania thin films on glass; active photocatalysts. Polyhedron, 2003, 22, 35-44.	2.2	150
52	Buoyancy increase and drag-reduction through a simple superhydrophobic coating. Nanoscale, 2017, 9, 7588-7594.	5.6	141
53	Solid state metathesis routes to transition metal carbides. Journal of Materials Chemistry, 1999, 9, 1275-1281.	6.7	138
54	A Dendritic Nickel Cobalt Sulfide Nanostructure for Alkaline Battery Electrodes. Advanced Functional Materials, 2018, 28, 1705937.	14.9	138

#	Article	IF	CITATIONS
55	Transient Absorption Spectroscopy of Anatase and Rutile: The Impact of Morphology and Phase on Photocatalytic Activity. Journal of Physical Chemistry C, 2015, 119, 10439-10447.	3.1	135
56	Exceptional supercapacitor performance from optimized oxidation of graphene-oxide. Energy Storage Materials, 2019, 17, 12-21.	18.0	135
57	Flexible and Selfâ€Powered Photodetector Arrays Based on Allâ€Inorganic CsPbBr ₃ Quantum Dots. Advanced Materials, 2020, 32, e2000004.	21.0	134
58	Selfâ€propagating highâ€ŧemperature synthesis of ferrites MFe2O4 (M = Mg, Ba, Co, Ni, Cu, Zn); reactions in an external magnetic field. Journal of Materials Chemistry, 1999, 9, 2545-2552.	6.7	129
59	Atmospheric pressure chemical vapor deposition of WSe2thin films on glass—highly hydrophobic sticky surfaces. Journal of Materials Chemistry, 2006, 16, 122-127.	6.7	128
60	Where Do Photogenerated Holes Go in Anatase:Rutile TiO ₂ ? A Transient Absorption Spectroscopy Study of Charge Transfer and Lifetime. Journal of Physical Chemistry A, 2016, 120, 715-723.	2.5	128
61	N ₂ Electroreduction to NH ₃ by Selenium Vacancyâ€Rich ReSe ₂ Catalysis at an Abrupt Interface. Angewandte Chemie - International Edition, 2020, 59, 13320-13327.	13.8	127
62	Carboxylic acid-stabilised iron oxide nanoparticles for use in magnetic hyperthermia. Journal of Materials Chemistry, 2009, 19, 6529.	6.7	126
63	Water droplet bouncing—a definition for superhydrophobic surfaces. Chemical Communications, 2011, 47, 12059.	4.1	125
64	Self-cleaning superhydrophobic surface based on titanium dioxide nanowires combined with polydimethylsiloxane. Applied Surface Science, 2013, 284, 319-323.	6.1	125
65	Creating robust superamphiphobic coatings for both hard and soft materials. Journal of Materials Chemistry A, 2015, 3, 20999-21008.	10.3	123
66	Tungsten Doped TiO2 with Enhanced Photocatalytic and Optoelectrical Properties via Aerosol Assisted Chemical Vapor Deposition. Scientific Reports, 2015, 5, 10952.	3.3	122
67	Carbonâ€Nanotube–PDMS Composite Coatings on Optical Fibers for Allâ€Optical Ultrasound Imaging. Advanced Functional Materials, 2016, 26, 8390-8396.	14.9	120
68	Multichannel Detection and Differentiation of Explosives with a Quantum Dot Array. ACS Nano, 2016, 10, 1139-1146.	14.6	120
69	Atmospheric pressure chemical vapour deposition of tungsten doped vanadium(iv) oxide from VOCl3, water and WCl6. Journal of Materials Chemistry, 2004, 14, 2554.	6.7	119
70	Large-Area Fabrication of Droplet Pancake Bouncing Surface and Control of Bouncing State. ACS Nano, 2017, 11, 9259-9267.	14.6	118
71	Copper as an antimicrobial agent: recent advances. RSC Advances, 2021, 11, 18179-18186.	3.6	118
72	Sulfurâ€Deficient Bismuth Sulfide/Nitrogenâ€Doped Carbon Nanofibers as Advanced Freeâ€Standing Electrode for Asymmetric Supercapacitors. Small, 2018, 14, e1801562.	10.0	117

#	Article	IF	CITATIONS
73	The first single source deposition of tin sulfide coatings on glass: aerosol-assisted chemical vapour deposition using [Sn(SCH2CH2S)2]. Journal of Materials Chemistry, 2001, 11, 1486-1490.	6.7	115
74	Evidence and Effect of Photogenerated Charge Transfer for Enhanced Photocatalysis in WO ₃ /TiO ₂ Heterojunction Films: A Computational and Experimental Study. Advanced Functional Materials, 2017, 27, 1605413.	14.9	115
75	Engineering Polymer Glue towards 90% Zinc Utilization for 1000 Hours to Make Highâ€Performance Znâ€Ion Batteries. Advanced Functional Materials, 2021, 31, 2107652.	14.9	115
76	Lethal photosensitisation of Staphylococcus aureus using a toluidine blue O–tiopronin–gold nanoparticle conjugate. Journal of Materials Chemistry, 2007, 17, 3739.	6.7	113
77	Multifunctional P-Doped TiO ₂ Films: A New Approach to Self-Cleaning, Transparent Conducting Oxide Materials. Chemistry of Materials, 2015, 27, 3234-3242.	6.7	113
78	Barrel‧haped Oil Skimmer Designed for Collection of Oil from Spills. Advanced Materials Interfaces, 2015, 2, 1500350.	3.7	112
79	Atmospheric pressure chemical vapour deposition of thermochromic tungsten doped vanadium dioxide thin films for use in architectural glazing. Thin Solid Films, 2009, 517, 4565-4570.	1.8	111
80	Recent Developments in the Field of Explosive Trace Detection. ACS Nano, 2020, 14, 10804-10833.	14.6	110
81	Titanium dioxide and composite metal/metal oxide titania thin films on glass: A comparative study of photocatalytic activity. Journal of Photochemistry and Photobiology A: Chemistry, 2009, 204, 183-190.	3.9	107
82	Porous biocompatible implants and tissue scaffolds synthesized by selective laser sintering from Ti and NiTi. Journal of Materials Chemistry, 2008, 18, 1309.	6.7	106
83	Enhanced photocatalytic activity under visible light in N-doped TiO2 thin films produced by APCVD preparations using t-butylamine as a nitrogen source and their potential for antibacterial films. Journal of Photochemistry and Photobiology A: Chemistry, 2009, 207, 244-253.	3.9	106
84	Ultrasmall CuCo ₂ S ₄ Nanocrystals: Allâ€inâ€One Theragnosis Nanoplatform with Magnetic Resonance/Nearâ€infrared Imaging for Efficiently Photothermal Therapy of Tumors. Advanced Functional Materials, 2017, 27, 1606218.	14.9	106
85	White light induced photocatalytic activity of sulfur-doped TiO2 thin films and their potential for antibacterial application. Journal of Materials Chemistry, 2009, 19, 8747.	6.7	105
86	Water Oxidation Kinetics of Accumulated Holes on the Surface of a TiO ₂ Photoanode: A Rate Law Analysis. ACS Catalysis, 2017, 7, 4896-4903.	11.2	105
87	CVD and precursor chemistry of transition metal nitrides. Coordination Chemistry Reviews, 2013, 257, 2073-2119.	18.8	102
88	Enhanced Photocatalytic and Antibacterial Ability of Cu-Doped Anatase TiO ₂ Thin Films: Theory and Experiment. ACS Applied Materials & Interfaces, 2020, 12, 15348-15361.	8.0	102
89	Highly conductive and transparent gallium doped zinc oxide thin films via chemical vapor deposition. Scientific Reports, 2020, 10, 638.	3.3	102
90	Cathode Design for Aqueous Rechargeable Multivalent Ion Batteries: Challenges and Opportunities. Advanced Functional Materials, 2021, 31, 2010445.	14.9	102

#	Article	IF	CITATIONS
91	Laser-generated ultrasound with optical fibres using functionalised carbon nanotube composite coatings. Applied Physics Letters, 2014, 104, .	3.3	101
92	Enabling stable MnO ₂ matrix for aqueous zinc-ion battery cathodes. Journal of Materials Chemistry A, 2020, 8, 22075-22082.	10.3	101
93	Enhanced transparent-conducting fluorine-doped tin oxide films formed by Aerosol-Assisted Chemical Vapour Deposition. Journal of Materials Chemistry C, 2013, 1, 984-996.	5.5	100
94	Nano-composite thermochromic thin films and their application in energy-efficient glazing. Solar Energy Materials and Solar Cells, 2010, 94, 141-151.	6.2	99
95	Graphene/nitrogen-doped porous carbon sandwiches for the metal-free oxygen reduction reaction: conductivity versus active sites. Journal of Materials Chemistry A, 2016, 4, 12658-12666.	10.3	99
96	Efficiently texturing hierarchical superhydrophobic fluoride-free translucent films by AACVD with excellent durability and self-cleaning ability. Journal of Materials Chemistry A, 2018, 6, 17633-17641.	10.3	99
97	Refining Energy Levels in ReS ₂ Nanosheets by Lowâ€Valent Transitionâ€Metal Doping for Dualâ€Boosted Electrochemical Ammonia/Hydrogen Production. Advanced Functional Materials, 2020, 30, 1907376.	14.9	99
98	Enhanced electrical properties of antimony doped tin oxide thin films deposited <i>via</i> aerosol assisted chemical vapour deposition. Journal of Materials Chemistry C, 2018, 6, 7257-7266.	5.5	97
99	Dualâ€Mechanism Antimicrobial Polymer–ZnO Nanoparticle and Crystal Violetâ€Encapsulated Silicone. Advanced Functional Materials, 2015, 25, 1367-1373.	14.9	94
100	Designing durable and flexible superhydrophobic coatings and its application in oil purification. Journal of Materials Chemistry A, 2016, 4, 4107-4116.	10.3	94
101	APCVD of thermochromic vanadium dioxide thin films—solid solutions V2–xMxO2 (M = Mo, Nb) or composites VO2 : SnO2. Journal of Materials Chemistry, 2005, 15, 4560.	6.7	93
102	Solution Processing Route to Multifunctional Titania Thin Films: Highly Conductive and Photcatalytically Active Nb:TiO ₂ . Advanced Functional Materials, 2014, 24, 5075-5085.	14.9	93
103	Synthesis and characterisation of W-doped VO2 by Aerosol Assisted Chemical Vapour Deposition. Thin Solid Films, 2008, 516, 1992-1997.	1.8	91
104	Fabrication of robust superhydrophobic surfaces <i>via</i> aerosol-assisted CVD and thermo-triggered healing of superhydrophobicity by recovery of roughness structures. Journal of Materials Chemistry A, 2019, 7, 17604-17612.	10.3	91
105	Topochemistryâ€Driven Synthesis of Transitionâ€Metal Selenides with Weakened Van Der Waals Force to Enable 3Dâ€Printed Naâ€Ion Hybrid Capacitors. Advanced Functional Materials, 2022, 32, .	14.9	91
106	A bioinspired solution for spectrally selective thermochromic VO_2 coated intelligent glazing. Optics Express, 2013, 21, A750.	3.4	90
107	Through-needle all-optical ultrasound imaging in vivo: a preclinical swine study. Light: Science and Applications, 2017, 6, e17103-e17103.	16.6	90
108	High-efficiency bubble transportation in an aqueous environment on a serial wedge-shaped wettability pattern. Journal of Materials Chemistry A, 2019, 7, 13567-13576.	10.3	90

#	Article	IF	CITATIONS
109	Highly Sensitive ZnO Nanorod- and Nanoprism-Based NO ₂ Gas Sensors: Size and Shape Control Using a Continuous Hydrothermal Pilot Plant. Langmuir, 2013, 29, 10603-10609.	3.5	89
110	Electrochemical sensor for discrimination tyrosine enantiomers using graphene quantum dots and β-cyclodextrins composites. Talanta, 2017, 173, 94-100.	5.5	89
111	Facile fabrication of stable superhydrophobic SiO2/polystyrene coating and separation of liquids with different surface tension. Chemical Engineering Journal, 2013, 231, 414-419.	12.7	88
112	Copper-based water repellent and antibacterial coatings by aerosol assisted chemical vapour deposition. Chemical Science, 2016, 7, 5126-5131.	7.4	87
113	The interaction between gold nanoparticles and cationic and anionic dyes: enhanced UV-visible absorption. Physical Chemistry Chemical Physics, 2009, 11, 10513.	2.8	86
114	Advances towards programmable droplet transport on solid surfaces and its applications. Chemical Society Reviews, 2020, 49, 7879-7892.	38.1	86
115	Transforming a Simple Commercial Glue into Highly Robust Superhydrophobic Surfaces via Aerosol-Assisted Chemical Vapor Deposition. ACS Applied Materials & Interfaces, 2017, 9, 42327-42335.	8.0	85
116	Antimicrobial activity of methylene blue and toluidine blue O covalently bound to a modified silicone polymer surface. Journal of Materials Chemistry, 2009, 19, 6167.	6.7	83
117	Shining light on materials — A self-sterilising revolution. Advanced Drug Delivery Reviews, 2013, 65, 570-580.	13.7	83
118	A superhydrophilic cement-coated mesh: an acid, alkali, and organic reagent-free material for oil/water separation. Nanoscale, 2018, 10, 1920-1929.	5.6	81
119	Polydimethylsiloxane Composites for Optical Ultrasound Generation and Multimodality Imaging. Advanced Functional Materials, 2018, 28, 1704919.	14.9	81
120	Aerosol assisted chemical vapour deposition of photochromic tungsten oxide and doped tungsten oxide thin films. Journal of Materials Chemistry, 2004, 14, 2864.	6.7	79
121	Chemical Vapor Deposition of Photocatalytically Active Pure Brookite TiO ₂ Thin Films. Chemistry of Materials, 2018, 30, 1353-1361.	6.7	79
122	Aerosol Assisted Chemical Vapor Deposition of Transparent Conductive Zinc Oxide Films. Chemistry of Materials, 2012, 24, 4704-4710.	6.7	78
123	Sensitive and specific detection of explosives in solution and vapour by surface-enhanced Raman spectroscopy on silver nanocubes. Nanoscale, 2017, 9, 16459-16466.	5.6	78
124	Nb-Doped VO2 Thin Films Prepared by Aerosol-Assisted Chemical Vapour Deposition. European Journal of Inorganic Chemistry, 2007, 2007, 4050-4055.	2.0	77
125	A general method for boosting the supercapacitor performance of graphitic carbon nitride/graphene hybrids. Journal of Materials Chemistry A, 2017, 5, 25545-25554.	10.3	77
126	Enhanced adsorption capacity of ultralong hydrogen titanate nanobelts for antibiotics. Journal of Materials Chemistry A, 2017, 5, 4352-4358.	10.3	76

#	Article	IF	CITATIONS
127	Tungsten Oxide Coatings from the Aerosol-Assisted Chemical Vapor Deposition of W(OAr)6(Ar = C6H5,) Tj ETQq1	1.0.7843 6.7	14 rgBT /0
128	Scalable route to CH ₃ NH ₃ PbI ₃ perovskite thin films by aerosol assisted chemical vapour deposition. Journal of Materials Chemistry A, 2015, 3, 9071-9073.	10.3	75
129	Super-durable, non-fluorinated superhydrophobic free-standing items. Journal of Materials Chemistry A, 2018, 6, 357-362.	10.3	75
130	Deposition of tin sulfide thin films from novel, volatile (fluoroalkythiolato)tin(iv) precursors. Journal of Materials Chemistry, 2001, 11, 469-473.	6.7	74
131	Spectral and photocatalytic characteristics of TiO2 CVD films on quartz. Photochemical and Photobiological Sciences, 2002, 1, 865-868.	2.9	74
132	Atmospheric pressure chemical vapour deposition of titanium dioxide coatings on glass. Journal of Materials Chemistry, 2003, 13, 56-60.	6.7	74
133	Vanadium(IV) oxide thin films on glass and silicon from the atmospheric pressure chemical vapour deposition reaction of VOCI3 and water. Polyhedron, 2004, 23, 3087-3095.	2.2	73
134	Antimicrobial activity of copper and copper(<scp>i</scp>) oxide thin films deposited via aerosol-assisted CVD. Journal of Materials Chemistry B, 2014, 2, 2855-2860.	5.8	73
135	The Role of Phosphate Group in Doped Cobalt Molybdate: Improved Electrocatalytic Hydrogen Evolution Performance. Advanced Science, 2020, 7, 1903674.	11.2	73
136	Anatase Thin Films on Glass from the Chemical Vapor Deposition of Titanium(IV) Chloride and Ethyl Acetate. Chemistry of Materials, 2003, 15, 46-50.	6.7	72
137	Underwater Spontaneous Pumpless Transportation of Nonpolar Organic Liquids on Extreme Wettability Patterns. ACS Applied Materials & Interfaces, 2016, 8, 2942-2949.	8.0	72
138	Aluminium/gallium, indium/gallium, and aluminium/indium co-doped ZnO thin films deposited <i>via</i> aerosol assisted CVD. Journal of Materials Chemistry C, 2018, 6, 588-597.	5.5	72
139	Synthesis and thermal decomposition studies of homo- and heteroleptic tin(iv) thiolates and dithiocarbamates: molecular precursors for tin sulfides. Dalton Transactions RSC, 2002, , 1085-1092.	2.3	71
140	Origin of High Mobility in Molybdenum-Doped Indium Oxide. Chemistry of Materials, 2015, 27, 2788-2796.	6.7	71
141	Potent Antibacterial Activity of Copper Embedded into Silicone and Polyurethane. ACS Applied Materials & amp; Interfaces, 2015, 7, 22807-22813.	8.0	71
142	Flexible and mechanically robust superhydrophobic silicone surfaces with stable Cassie–Baxter state. Journal of Materials Chemistry A, 2016, 4, 14180-14186.	10.3	71
143	Optimizing the Activity of Nanoneedle Structured WO ₃ Photoanodes for Solar Water Splitting: Direct Synthesis via Chemical Vapor Deposition. Journal of Physical Chemistry C, 2017, 121, 5983-5993.	3.1	71
144	Robust platform for water harvesting and directional transport. Journal of Materials Chemistry A, 2018, 6, 5635-5643.	10.3	71

#	Article	IF	CITATIONS
145	Identification and manipulation of dynamic active site deficiency-induced competing reactions in electrocatalytic oxidation processes. Energy and Environmental Science, 2022, 15, 2386-2396.	30.8	71
146	Rationally Designed Sodium Chromium Vanadium Phosphate Cathodes with Multiâ€Electron Reaction for Fastâ€Charging Sodiumâ€Ion Batteries. Advanced Energy Materials, 2022, 12, .	19.5	71
147	Intrinsic intermediate gap states of TiO2 materials and their roles in charge carrier kinetics. Journal of Photochemistry and Photobiology C: Photochemistry Reviews, 2019, 39, 1-57.	11.6	70
148	Solid state metathesis: synthesis of metal carbides from metal oxides. Journal of Materials Chemistry, 2001, 11, 3116-3119.	6.7	69
149	Zinc Oxide Thin Films Grown by Aerosol Assisted CVD. Chemical Vapor Deposition, 2008, 14, 366-372.	1.3	69
150	Nanoparticulate silver coated-titania thin films—Photo-oxidative destruction of stearic acid under different light sources and antimicrobial effects under hospital lighting conditions. Journal of Photochemistry and Photobiology A: Chemistry, 2011, 220, 113-123.	3.9	69
151	The vapour phase detection of explosive markers and derivatives using two fluorescent metal–organic frameworks. Journal of Materials Chemistry A, 2015, 3, 6351-6359.	10.3	69
152	Progress and Perspectives of Organosulfur for Lithium–Sulfur Batteries. Advanced Energy Materials, 2022, 12, 2103483.	19.5	69
153	Continuous flow synthesis of ultrasmall gold nanoparticles in a microreactor using trisodium citrate and their SERS performance. Chemical Engineering Science, 2018, 189, 422-430.	3.8	68
154	Atmospheric pressure chemical vapour deposition of WS2 thin films on glass. Polyhedron, 2003, 22, 1499-1505.	2.2	67
155	Gallium Oxide Thin Films from the Atmospheric Pressure Chemical Vapor Deposition Reaction of Gallium Trichloride and Methanol. Chemistry of Materials, 2004, 16, 2489-2493.	6.7	67
156	The Use of Combinatorial Chemical Vapor Deposition in the Synthesis of Ti ₃ ₋ _{{´} O ₄ N with 0.06 < δ < 0.25:  A Titanium Oxynitri Phase Isostructural to Anosovite. Journal of the American Chemical Society, 2007, 129, 15541-15548.	de13.7	67
157	Microstructure and antibacterial efficacy of graphene oxide nanocomposite fibres. Journal of Colloid and Interface Science, 2020, 571, 239-252.	9.4	67
158	New routes to alkali-metal–rare-earth-metal sulfides. Journal of Materials Chemistry, 1994, 4, 1603-1609.	6.7	66
159	Deposition of tin sulfide thin films from tin(iv) thiolate precursors. Journal of Materials Chemistry, 2001, 11, 464-468.	6.7	65
160	X-ray Diffraction Area Mapping of Preferred Orientation and Phase Change in TiO2Thin Films Deposited by Chemical Vapor Deposition. Journal of the American Chemical Society, 2006, 128, 12147-12155.	13.7	65
161	High-Throughput Continuous Hydrothermal Synthesis of an Entire Nanoceramic Phase Diagram. ACS Combinatorial Science, 2009, 11, 829-834.	3.3	65
162	Antimicrobial activity of polyurethane embedded with methylene blue, toluidene blue and gold nanoparticles against Staphylococcus aureus; illuminated with white light. Materials Chemistry and Physics, 2011, 129, 446-450.	4.0	65

#	Article	IF	CITATIONS
163	A novel damage-tolerant superhydrophobic and superoleophilic material. Journal of Materials Chemistry A, 2014, 2, 9002-9006.	10.3	65
164	Aerosol assisted chemical vapour deposition of WO3 thin films from tungsten hexacarbonyl and their gas sensing properties. Journal of Materials Chemistry, 2007, 17, 3708.	6.7	64
165	Atmospheric pressure chemical vapour deposition of vanadium diselenide thin films. Applied Surface Science, 2007, 253, 6041-6046.	6.1	64
166	Enhanced performance of ZnO nanoparticle decorated all-inorganic CsPbBr ₃ quantum dot photodetectors. Journal of Materials Chemistry A, 2019, 7, 6134-6142.	10.3	64
167	Resonant doping for high mobility transparent conductors: the case of Mo-doped In ₂ O ₃ . Materials Horizons, 2020, 7, 236-243.	12.2	64
168	Macroscale Superlubricity Enabled by Graphene oated Surfaces. Advanced Science, 2020, 7, 1903239.	11.2	64
169	Investigation of a Biomass Hydrogel Electrolyte Naturally Stabilizing Cathodes for Zinc-Ion Batteries. ACS Applied Materials & Interfaces, 2021, 13, 745-754.	8.0	64
170	Ultra-stretchable and superhydrophobic textile-based bioelectrodes for robust self-cleaning and personal health monitoring. Nano Energy, 2022, 97, 107160.	16.0	64
171	Aerosol Assisted Chemical Vapor Deposition of Gold and Nanocomposite Thin Films from Hydrogen Tetrachloroaurate(III). Chemistry of Materials, 2007, 19, 4639-4647.	6.7	63
172	Ambient Fabrication of Organic–Inorganic Hybrid Perovskite Solar Cells. Small Methods, 2021, 5, e2000744.	8.6	63
173	Antibacterial Activity of Light-Activated Silicone Containing Methylene Blue and Gold Nanoparticles of Different Sizes. Journal of Cluster Science, 2010, 21, 427-438.	3.3	62
174	Incorporation of methylene blue and nanogold into polyvinyl chloride catheters; a new approach for light-activated disinfection of surfaces. Journal of Materials Chemistry, 2012, 22, 15388.	6.7	62
175	A novel bone cement impregnated with silver–tiopronin nanoparticles: its antimicrobial, cytotoxic, and mechanical properties. International Journal of Nanomedicine, 2013, 8, 2227.	6.7	62
176	Unprecedented Piezoresistance Coefficient in Strained Silicon Carbide. Nano Letters, 2019, 19, 6569-6576.	9.1	62
177	Dynamics of Photoâ€Induced Surface Oxygen Vacancies in Metalâ€Oxide Semiconductors Studied Under Ambient Conditions. Advanced Science, 2019, 6, 1901841.	11.2	62
178	Tantalum and Titanium doped In ₂ O ₃ Thin Films by Aerosol-Assisted Chemical Vapor Deposition and their Gas Sensing Properties. Chemistry of Materials, 2012, 24, 2864-2871.	6.7	61
179	Defected vanadium bronzes as superb cathodes in aqueous zinc-ion batteries. Nanoscale, 2020, 12, 20638-20648.	5.6	61
180	Synthesis of Titanium(IV) Guanidinate Complexes and the Formation of Titanium Carbonitride via Low-Pressure Chemical Vapor Deposition. Inorganic Chemistry, 2005, 44, 615-619.	4.0	60

#	Article	IF	CITATIONS
181	The combinatorial atmospheric pressure chemical vapour deposition (cAPCVD) of a gradating substitutional/interstitial N-doped anatase TiO2 thin-film; UVA and visible light photocatalytic activities. Journal of Photochemistry and Photobiology A: Chemistry, 2010, 216, 156-166.	3.9	60
182	Toluidine blue-containing polymers exhibit potent bactericidal activity when irradiated with red laser light. Journal of Materials Chemistry, 2009, 19, 2715.	6.7	59
183	Aerosol-Assisted Chemical Vapor Deposition of Transparent Conductive Galliumâ^'Indiumâ^'Oxide Films. Chemistry of Materials, 2011, 23, 1719-1726.	6.7	59
184	Oxygen vacancy engineering in spinel-structured nanosheet wrapped hollow polyhedra for electrochemical nitrogen fixation under ambient conditions. Journal of Materials Chemistry A, 2020, 8, 1652-1659.	10.3	59
185	Atmospheric pressure chemical vapour deposition of VO2 and VO2/TiO2 films from the reaction of VOCl3, TiCl4 and water. Journal of Materials Chemistry, 2004, 14, 1190.	6.7	58
186	Copperâ€Doped CdSe/ZnS Quantum Dots: Controllable Photoactivated Copper(I) Cation Storage and Release Vectors for Catalysis. Angewandte Chemie - International Edition, 2014, 53, 1598-1601.	13.8	58
187	Dynamic Control of Particle Deposition in Evaporating Droplets by an External Point Source of Vapor. Journal of Physical Chemistry Letters, 2018, 9, 659-664.	4.6	58
188	A Universal Polyiodide Regulation Using Quaternization Engineering toward High Valueâ€Added and Ultra‣table Zinc″odine Batteries. Advanced Science, 2022, 9, e2105598.	11.2	58
189	Aerosol-assisted chemical vapour deposition of WO3 thin films using polyoxometallate precursors and their gas sensing properties. Journal of Materials Chemistry, 2007, 17, 1063.	6.7	57
190	Calcium phosphate-based materials of natural origin showing photocatalytic activity. Journal of Materials Chemistry A, 2013, 1, 6452.	10.3	57
191	Room temperature vanadium dioxide–carbon nanotube gas sensors made via continuous hydrothermal flow synthesis. Sensors and Actuators B: Chemical, 2018, 255, 1119-1129.	7.8	57
192	Visible light photocatalysts—N-doped TiO2 by sol–gel, enhanced with surface bound silver nanoparticle islands. Journal of Materials Chemistry, 2011, 21, 11854.	6.7	56
193	Textured Fluorineâ€Doped Tin Dioxide Films formed by Chemical Vapour Deposition. Chemistry - A European Journal, 2011, 17, 11613-11621.	3.3	56
194	Optimized Atmospheric-Pressure Chemical Vapor Deposition Thermochromic VO ₂ Thin Films for <i>Intelligent</i> Window Applications. ACS Omega, 2017, 2, 1040-1046.	3.5	56
195	Robust Superhydrophobic Conical Pillars from Syringe Needle Shape to Straight Conical Pillar Shape for Droplet Pancake Bouncing. ACS Applied Materials & Interfaces, 2019, 11, 45345-45353.	8.0	56
196	Natural Clayâ€Based Materials for Energy Storage and Conversion Applications. Advanced Science, 2021, 8, e2004036.	11.2	56
197	Aerosol assisted chemical vapour deposition of MoO3 and MoO2 thin films on glass from molybdenum polyoxometallate precursors; thermophoresis and gas phase nanoparticle formation. Journal of Materials Chemistry, 2006, 16, 3575.	6.7	55
198	Aerosol assisted chemical vapour deposition of hydrophobic TiO2–SnO2 composite film with novel microstructure and enhanced photocatalytic activity. Journal of Materials Chemistry A, 2013, 1, 6271.	10.3	55

#	Article	IF	CITATIONS
199	Combinatorial Atmospheric Pressure Chemical Vapor Deposition (cAPCVD): A Route to Functional Property Optimization. Journal of the American Chemical Society, 2011, 133, 20458-20467.	13.7	54
200	Self-assembly of metallic nanoparticles into one dimensional arrays. Journal of Materials Chemistry A, 2013, 1, 6985.	10.3	54
201	Thiol-Capped Gold Nanoparticles Swell-Encapsulated into Polyurethane as Powerful Antibacterial Surfaces Under Dark and Light Conditions. Scientific Reports, 2016, 6, 39272.	3.3	54
202	Chemical Vapor Deposition Synthesis and Optical Properties of Nb ₂ O ₅ Thin Films with Hybrid Functional Theoretical Insight into the Band Structure and Band Gaps. ACS Applied Materials & Interfaces, 2017, 9, 18031-18038.	8.0	54
203	Optical fiber ultrasound transmitter with electrospun carbon nanotube-polymer composite. Applied Physics Letters, 2017, 110, 223701.	3.3	54
204	Ultrahigh Recovery of Fracture Strength on Mismatched Fractured Amorphous Surfaces of Silicon Carbide. ACS Nano, 2019, 13, 7483-7492.	14.6	54
205	Sensing and Discrimination of Explosives at Variable Concentrations with a Large-Pore MOF as Part of a Luminescent Array. ACS Applied Materials & amp; Interfaces, 2019, 11, 11618-11626.	8.0	54
206	The applicability of high-speed counter current chromatography to the separation of natural antioxidants. Journal of Chromatography A, 2020, 1623, 461150.	3.7	54
207	Aerosol assisted chemical vapour deposition of tungsten oxide films from polyoxotungstate precursors: active photocatalysts. Chemical Communications, 2003, , 1696.	4.1	53
208	Damaging and protective properties of inorganic components of sunscreens applied to cultured human skin cells. Journal of Photochemistry and Photobiology A: Chemistry, 2007, 191, 138-148.	3.9	53
209	Combinatorial atmospheric pressure chemical vapour deposition (cAPCVD) of niobium doped anatase; effect of niobium on the conductivity and photocatalytic activity. Journal of Materials Chemistry, 2010, 20, 8336.	6.7	53
210	Combinatorial Atmospheric Pressure Chemical Vapor Deposition of Graded TiO ₂ –VO ₂ Mixed-Phase Composites and Their Dual Functional Property as Self-Cleaning and Photochromic Window Coatings. ACS Combinatorial Science, 2013, 15, 309-319.	3.8	53
211	Synergistic relationship between the three-dimensional nanostructure and electrochemical performance in biocarbon supercapacitor electrode materials. Sustainable Energy and Fuels, 2018, 2, 772-785.	4.9	53
212	Zeolite-modified WO3 gas sensors – Enhanced detection of NO2. Sensors and Actuators B: Chemical, 2011, 160, 475-482.	7.8	52
213	Light-activated antimicrobial surfaces with enhanced efficacy induced by a dark-activated mechanism. Chemical Science, 2014, 5, 2216-2223.	7.4	52
214	Self-standing electrodes with core-shell structures for high-performance supercapacitors. Energy Storage Materials, 2017, 9, 119-125.	18.0	52
215	Transparent superhydrophobic PTFE films via one-step aerosol assisted chemical vapor deposition. RSC Advances, 2017, 7, 29275-29283.	3.6	52
216	Energy level engineering in transition-metal doped spinel-structured nanosheets for efficient overall water splitting. Journal of Materials Chemistry A, 2019, 7, 827-833.	10.3	52

#	Article	IF	CITATIONS
217	Photobactericidal activity activated by thiolated gold nanoclusters at low flux levels of white light. Nature Communications, 2020, 11, 1207.	12.8	52
218	High efficiency water splitting photoanodes composed of nano-structured anatase-rutile TiO2 heterojunctions by pulsed-pressure MOCVD. Applied Catalysis B: Environmental, 2018, 224, 904-911.	20.2	51
219	PbO-Modified TiO ₂ Thin Films: A Route to Visible Light Photocatalysts. Langmuir, 2014, 30, 624-630.	3.5	50
220	A Method for Synthesis of Renewable Cu ₂ O Junction Composite Electrodes and Their Photoelectrochemical Properties. ACS Sustainable Chemistry and Engineering, 2015, 3, 710-717.	6.7	50
221	An array of WO ₃ and CTO heterojunction semiconducting metal oxide gas sensors used as a tool for explosive detection. Journal of Materials Chemistry A, 2017, 5, 2172-2179.	10.3	50
222	Resonant Ta Doping for Enhanced Mobility in Transparent Conducting SnO ₂ . Chemistry of Materials, 2020, 32, 1964-1973.	6.7	50
223	A single step route to superhydrophobic surfaces through aerosol assisted deposition of rough polymer surfaces: duplicating the lotus effect. Journal of Materials Chemistry, 2009, 19, 1074-1076.	6.7	49
224	Zeolite-Modified Discriminating Gas Sensors. Journal of the Electrochemical Society, 2009, 156, J46.	2.9	49
225	Low-temperature routes to early transition-metal nitrides. Journal of the Chemical Society Dalton Transactions, 1993, , 2435.	1.1	48
226	Atmospheric Pressure Chemical Vapour Deposition of NbSe2 Thin Films on Glass. European Journal of Inorganic Chemistry, 2006, 2006, 1255-1259.	2.0	48
227	The combinatorial atmospheric pressure chemical vapour deposition (cAPCVD) of a gradating N-doped mixed phase titania thin film. Journal of Materials Chemistry, 2010, 20, 2157.	6.7	48
228	CVD of copper and copper oxide thin films via the in situ reduction of copper(ii) nitrate—a route to conformal superhydrophobic coatings. Journal of Materials Chemistry, 2011, 21, 14712.	6.7	48
229	Nanoparticles Encapsulated in Porous Carbon Matrix Coated on Carbon Fibers: An Ultrastable Cathode for Liâ€lon Batteries. Advanced Energy Materials, 2017, 7, 1601363.	19.5	48
230	Rapid, Solid-State Metathesis Routes to Metal Carbides. Advanced Materials, 1998, 10, 805-808.	21.0	47
231	Atmospheric pressure chemical vapour deposition of tin(ii) sulfide films on glass substrates from Bun3SnO2CCF3 with hydrogen sulfide. Journal of Materials Chemistry, 2000, 10, 527-530.	6.7	47
232	Title is missing!. Journal of Materials Chemistry, 2001, 11, 3120-3124.	6.7	47
233	A general method for the incorporation of nanoparticles into superhydrophobic films by aerosol assisted chemical vapour deposition. Journal of Materials Chemistry A, 2013, 1, 4336.	10.3	47
234	Direct and continuous synthesis of VO ₂ nanoparticles. Nanoscale, 2015, 7, 18686-18693.	5.6	47

#	Article	IF	CITATIONS
235	All-Optical Rotational Ultrasound Imaging. Scientific Reports, 2019, 9, 5576.	3.3	47
236	Adsorption of volatile organic compounds by industrial porous materials: Impact of relative humidity. Microporous and Mesoporous Materials, 2020, 298, 110090.	4.4	47
237	Thermochromic Coatings for Intelligent Architectural Glazing. Journal of Nano Research, 0, 2, 1-20.	0.8	46
238	Transparent conducting n-type ZnO:Sc – synthesis, optoelectronic properties and theoretical insight. Journal of Materials Chemistry C, 2017, 5, 7585-7597.	5.5	46
239	Superhydrophilic–superhydrophobic patterned surfaces on glass substrate for water harvesting. Journal of Materials Science, 2020, 55, 498-508.	3.7	46
240	Combinatorial atmospheric pressure chemical vapour deposition (cAPCVD) of a mixed vanadium oxide and vanadium oxynitride thin film. Journal of Materials Chemistry, 2009, 19, 1399.	6.7	45
241	Does a Photocatalytic Synergy in an Anatase–Rutile TiO ₂ Composite Thinâ€Film Exist?. Chemistry - A European Journal, 2012, 18, 13048-13058.	3.3	45
242	Water droplets bouncing on superhydrophobic soft porous materials. Journal of Materials Chemistry A, 2014, 2, 12177-12184.	10.3	45
243	Phase and morphological control of MoO _{3â^'x} nanostructures for efficient cancer theragnosis therapy. Nanoscale, 2017, 9, 11012-11016.	5.6	45
244	Origin of Performance Enhancement in TiO ₂ arbon Nanotube Composite Perovskite Solar Cells. Small Methods, 2019, 3, 1900164.	8.6	45
245	Bandwidth limits of luminescent solar concentrators as detectors in free-space optical communication systems. Light: Science and Applications, 2021, 10, 3.	16.6	45
246	Facile Fabrication of Robust Hydrogen Evolution Electrodes under High Current Densities via Pt@Cu Interactions. Advanced Functional Materials, 2021, 31, 2105579.	14.9	45
247	Gallium oxide thin films from the AACVD of [Ga(NMe2)3]2 and donor functionalised alcohols. Dalton Transactions, 2008, , 591.	3.3	44
248	Inorganic thin-film combinatorial studies for rapidly optimising functional properties. Chemical Society Reviews, 2012, 41, 738-781.	38.1	44
249	Combinatorial Atmospheric Pressure Chemical Vapor Deposition of F:TiO ₂ ; the Relationship between Photocatalysis and Transparent Conducting Oxide Properties. Advanced Functional Materials, 2014, 24, 1758-1771.	14.9	44
250	Critical influence of surface nitrogen species on the activity of N-doped TiO2 thin-films during photodegradation of stearic acid under UV light irradiation. Applied Catalysis B: Environmental, 2014, 160-161, 582-588.	20.2	44
251	Interstitial Boron-Doped TiO ₂ Thin Films: The Significant Effect of Boron on TiO ₂ Coatings Grown by Atmospheric Pressure Chemical Vapor Deposition. ACS Applied Materials & Interfaces, 2016, 8, 25024-25029.	8.0	44
252	Scaling aerosol assisted chemical vapour deposition: Exploring the relationship between growth rate and film properties. Materials and Design, 2017, 129, 116-124.	7.0	44

#	Article	IF	CITATIONS
253	New Insights into the Fundamental Principle of Semiconductor Photocatalysis. ACS Omega, 2020, 5, 14847-14856.	3.5	44
254	Synthesis of TiN thin films from titanium imido complexes. Journal of Materials Chemistry, 2003, 13, 84-87.	6.7	43
255	Tungsten doped vanadium dioxide thin films prepared by atmospheric pressure chemical vapour deposition from vanadyl acetylacetonate and tungsten hexachloride. Surface and Coatings Technology, 2007, 201, 9369-9372.	4.8	43
256	Gold Nanoparticles Enhance the Toluidine Blue-Induced Lethal Photosensitisation of Staphylococcus aureus. Current Nanoscience, 2008, 4, 409-414.	1.2	43
257	Nanostructured tungsten oxide gas sensors prepared by electric field assisted aerosol assisted chemical vapour deposition. Journal of Materials Chemistry A, 2013, 1, 1827-1833.	10.3	43
258	Photocatalytic Evidence of the Rutileâ€ŧoâ€Anatase Electron Transfer in Titania. Advanced Materials Interfaces, 2014, 1, 1400069.	3.7	43
259	The gas sensing properties of zeolite modified zinc oxide. Journal of Materials Chemistry A, 2014, 2, 4758-4764.	10.3	43
260	Lethal photosensitisation of Staphylococcus aureus and Escherichia coli using crystal violet and zinc oxide-encapsulated polyurethane. Journal of Materials Chemistry B, 2015, 3, 6490-6500.	5.8	43
261	Alâ€, Gaâ€, and Inâ€doped ZnO thin films via aerosol assisted CVD for use as transparent conducting oxides. Physica Status Solidi (A) Applications and Materials Science, 2016, 213, 1346-1352.	1.8	43
262	Multi-mode application of graphene quantum dots bonded silica stationary phase for high performance liquid chromatography. Journal of Chromatography A, 2017, 1492, 61-69.	3.7	43
263	A simple equivalent circuit model to represent microstructure effects on the response of semiconducting oxide-based gas sensors. Measurement Science and Technology, 2003, 14, 76-86.	2.6	42
264	Formation of a new (1T) trigonal NbS2 polytype via atmospheric pressure chemical vapour depositionElectronic supplementary information (ESI) available: structure refinements of the NbS2 films and crystallographic data in CIF format. See http://www.rsc.org/suppdata/jm/b3/b315782m/. Journal of Materials Chemistry, 2004, 14, 290.	6.7	42
265	Photobactericidal polymers; the incorporation of crystal violet and nanogold into medical grade silicone. RSC Advances, 2013, 3, 18383.	3.6	42
266	Transparent conductive aluminium and fluorine co-doped zinc oxide films via aerosol assisted chemical vapour deposition. RSC Advances, 2014, 4, 49723-49728.	3.6	42
267	Aerosol assisted chemical vapor deposition of conductive and photocatalytically active tantalum doped titanium dioxide films. Journal of Materials Chemistry A, 2014, 2, 12849.	10.3	42
268	Electrochemical fabrication of superhydrophobic Zn surfaces. Applied Surface Science, 2014, 315, 346-352.	6.1	42
269	ZnO Rods with Exposed {100} Facets Grown via a Self-Catalyzed Vapor–Solid Mechanism and Their Photocatalytic and Gas Sensing Properties. ACS Applied Materials & Interfaces, 2016, 8, 33335-33342.	8.0	42
270	Combined Effect of Temperature Induced Strain and Oxygen Vacancy on Metalâ€Insulator Transition of VO ₂ Colloidal Particles. Advanced Functional Materials, 2020, 30, 2005311.	14.9	42

#	Article	IF	CITATIONS
271	Supersaturated bridge-sulfur and vanadium co-doped M0S2 nanosheet arrays with enhanced sodium storage capability. Nano Research, 2021, 14, 74-80.	10.4	42
272	Sodium azide as a reagent for solid state metathesis preparations of refractory metal nitrides. Polyhedron, 1995, 14, 913-917.	2.2	41
273	Atmospheric pressure chemical vapour deposition of vanadium(v) oxide films on glass substrates from reactions of VOCl3 and VCl4 with water. Journal of Materials Chemistry, 2000, 10, 1863-1866.	6.7	41
274	Metal oxide semiconductor gas sensors utilizing a Cr-zeolite catalytic layer for improved selectivity. Measurement Science and Technology, 2005, 16, 1193-1200.	2.6	41
275	Simple method for the rapid simultaneous screening of photocatalytic activity over multiple positions of self-cleaning films. Physical Chemistry Chemical Physics, 2009, 11, 8367.	2.8	41
276	Electric field-assisted levitation-jet aerosol synthesis of Ni/NiO nanoparticles. Journal of Materials Chemistry, 2012, 22, 11214.	6.7	41
277	Enhancing the Antibacterial Activity of Light-Activated Surfaces Containing Crystal Violet and ZnO Nanoparticles: Investigation of Nanoparticle Size, Capping Ligand, and Dopants. ACS Omega, 2016, 1, 334-343.	3.5	41
278	Facile fabrication of durable superhydrophobic SiO ₂ /polyurethane composite sponge for continuous separation of oil from water. RSC Advances, 2017, 7, 11362-11366.	3.6	41
279	Aerosol-assisted chemical vapour deposition of transparent superhydrophobic film by using mixed functional alkoxysilanes. Scientific Reports, 2019, 9, 7549.	3.3	41
280	An anti-aging polymer electrolyte for flexible rechargeable zinc-ion batteries. Journal of Materials Chemistry A, 2020, 8, 22637-22644.	10.3	41
281	High-Performance Zinc–Air Batteries with Scalable Metal–Organic Frameworks and Platinum Carbon Black Bifunctional Catalysts. ACS Applied Materials & Interfaces, 2020, 12, 42696-42703.	8.0	41
282	Self-propagating high-temperature synthesis of lithium-chromium ferrites Li0.5Fe2.5-xCrxO4. Journal Physics D: Applied Physics, 1998, 31, 2886-2893.	2.8	40
283	Atmospheric pressure chemical vapour deposition of thin films of Nb2O5 on glass. Journal of Materials Chemistry, 2003, 13, 2952.	6.7	40
284	Single-walled carbon nanotube composite inks for printed gas sensors: enhanced detection of NO ₂ , NH ₃ , EtOH and acetone. RSC Advances, 2014, 4, 51395-51403.	3.6	40
285	altimg="si1.svg"> <mml:mrow><mml:msub><mml:mrow><mml:mtext>VO</mml:mtext></mml:mrow><mml:mrce linebreak="goodbreak" linebreakstyle="after">â^<mml:msub><mml:mrow><mml:mtext>SiO</mml:mtext></mml:mrow><m nanocomposite smart window coatings with narrow phase transition hysteresis and transition</m </mml:msub></mml:mrce </mml:msub></mml:mrow>		
286	gradient width. Solar Energy Materials and Solar Cells, 2019, 200, 109944. Titanium sulfide thin films from the aerosol-assisted chemical vapour deposition of [Ti(SBut)4]. Journal of Materials Chemistry, 2004, 14, 830.	6.7	39
287	Plasmonic Gold Nanostars Incorporated into Highâ€Efficiency Perovskite Solar Cells. ChemSusChem, 2017, 10, 3750-3753.	6.8	39
288	The effect of solvent on Al-doped ZnO thin films deposited <i>via</i> aerosol assisted CVD. RSC Advances, 2018, 8, 33164-33173.	3.6	39

#	Article	IF	CITATIONS
289	Durable fire retardant, superhydrophobic, abrasive resistant and air/UV stable coatings. Journal of Colloid and Interface Science, 2021, 582, 301-311.	9.4	39
290	The bionic sunflower: a bio-inspired autonomous light tracking photocatalytic system. Energy and Environmental Science, 2021, 14, 3931-3937.	30.8	39
291	The extended time evolution size decrease of gold nanoparticles formed by the Turkevich method. New Journal of Chemistry, 2010, 34, 1401.	2.8	38
292	Superhydrophobic Surfaces as an On-Chip Microfluidic Toolkit for Total Droplet Control. Analytical Chemistry, 2013, 85, 5405-5410.	6.5	38
293	Cobalt nickel nitride coated by a thin carbon layer anchoring on nitrogen-doped carbon nanotube anodes for high-performance lithium-ion batteries. Journal of Materials Chemistry A, 2018, 6, 19853-19862.	10.3	38
294	Slippery Liquid Infused Porous TiO ₂ /SnO ₂ Nanocomposite Thin Films via Aerosol Assisted Chemical Vapor Deposition with Anti-Icing and Fog Retardant Properties. ACS Applied Materials & Interfaces, 2019, 11, 41804-41812.	8.0	38
295	Control of semiconducting oxide gas-sensor microstructure by application of an electric field during aerosol-assisted chemical vapour deposition. Journal of Materials Chemistry, 2005, 15, 149.	6.7	37
296	The effect of initiation method on the size, monodispersity and shape of gold nanoparticles formed by the Turkevich method. New Journal of Chemistry, 2010, 34, 2906.	2.8	37
297	Mesoporous silica-supported copper-catalysts for homocoupling reaction of terminal alkynes at room-temperature. New Journal of Chemistry, 2013, 37, 1343.	2.8	37
298	N-doped TiO2 visible light photocatalyst films via a sol–gel route using TMEDA as the nitrogen source. Journal of Photochemistry and Photobiology A: Chemistry, 2014, 281, 27-34.	3.9	37
299	The interaction of gold and silver nanoparticles with a range of anionic and cationic dyes. Physical Chemistry Chemical Physics, 2014, 16, 6050-6059.	2.8	37
300	Thermally-induced all-damage-healable superhydrophobic surface with photocatalytic performance from hierarchical BiOCl. Chemical Engineering Journal, 2019, 366, 439-448.	12.7	37
301	The anhydrous alums as model triangular-lattice magnets. Journal of Physics Condensed Matter, 1996, 8, L123-L129.	1.8	36
302	Solvent free reactions in the solid state: solid state metathesis. Transition Metal Chemistry, 2002, 27, 569-573.	1.4	36
303	The relationship between photocatalytic activity and photochromic state of nanoparticulate silver surface loaded titanium dioxide thin-films. Physical Chemistry Chemical Physics, 2011, 13, 13827.	2.8	36
304	Detection of explosive markers using zeolite modified gas sensors. Journal of Materials Chemistry A, 2013, 1, 2613.	10.3	36
305	Structure of Gold–Silver Nanoparticles. Journal of Physical Chemistry C, 2017, 121, 1957-1963.	3.1	36
306	Transparent conducting oxide thin films of Si-doped ZnO prepared by aerosol assisted CVD. RSC Advances, 2017, 7, 10806-10814.	3.6	36

#	Article	IF	CITATIONS
307	Continuous flow synthesis of citrate capped gold nanoparticles using UV induced nucleation. RSC Advances, 2017, 7, 9632-9638.	3.6	36
308	Microspheres of the gas sensor material Cr2 â^' xTixO3 prepared by the sol–emulsion–gel route. Journal of Materials Chemistry, 2001, 11, 1651-1655.	6.7	35
309	Titanium imido complexes as precursors to titanium nitride. Dalton Transactions RSC, 2002, , 4055-4059.	2.3	35
310	CuO three-dimensional flowerlike nanostructures: Controlled synthesis and characterization. Journal of Applied Physics, 2008, 103, .	2.5	35
311	Aerosolâ€Assisted CVD of Titanium Dioxide Thin Films from Methanolic Solutions of Titanium Tetraisopropoxide; Substrate and Aerosolâ€Selective Deposition of Rutile or Anatase. Chemical Vapor Deposition, 2011, 17, 30-36.	1.3	35
312	CVD Production of Doped Titanium Dioxide Thin Films. Chemical Vapor Deposition, 2012, 18, 89-101.	1.3	35
313	Assessing the potential of metal oxide semiconducting gas sensors for illicit drug detection markers. Journal of Materials Chemistry A, 2014, 2, 8952-8960.	10.3	35
314	Nanoparticle–sulphur "inverse vulcanisation―polymer composites. Chemical Communications, 2015, 51, 10467-10470.	4.1	35
315	Hydrophilic patterning of superhydrophobic surfaces by atmosphericâ€pressure plasma jet. Micro and Nano Letters, 2015, 10, 105-108.	1.3	35
316	CulnS ₂ /ZnS nanocrystals as sensitisers for NiO photocathodes. Journal of Materials Chemistry A, 2015, 3, 13324-13331.	10.3	35
317	Covalently Attached Antimicrobial Surfaces Using BODIPY: Improving Efficiency and Effectiveness. ACS Applied Materials & Interfaces, 2018, 10, 98-104.	8.0	35
318	Fabrication and characterization of degradable and durable fluoride-free super-hydrophobic cotton fabrics for oil/water separation. Surface and Coatings Technology, 2019, 378, 125079.	4.8	35
319	<i>In vivo</i> and <i>in vitro</i> efficient textile wastewater remediation by <i>Aspergillus niger</i> biosorbent. Nanoscale Advances, 2019, 1, 168-176.	4.6	35
320	Rapid synthesis of gold nanoparticles with carbon monoxide in a microfluidic segmented flow system. Reaction Chemistry and Engineering, 2019, 4, 884-890.	3.7	35
321	Chromium nitrides (CrN, Cr2N) from solid state metathesis reactions: effects of dilution and nitriding reagent. Journal of Materials Chemistry, 1998, 8, 1875-1880.	6.7	34
322	The APCVD of tungsten oxide thin films from reaction of WCl6 with ethanol and results on their gas-sensing properties. Polyhedron, 2007, 26, 1493-1498.	2.2	34
323	Sulfur―and Nitrogenâ€Doped Titania Biomaterials via APCVD. Chemical Vapor Deposition, 2010, 16, 50-54.	1.3	34
324	Discrimination Effects in Zeolite Modified Metal Oxide Semiconductor Gas Sensors. IEEE Sensors Journal, 2011, 11, 1145-1151.	4.7	34

#	Article	IF	CITATIONS
325	Photocatalytic activity of needle-like TiO2/WO3â^'x thin films prepared by chemical vapour deposition. Journal of Photochemistry and Photobiology A: Chemistry, 2012, 239, 60-64.	3.9	34
326	Influencing FTO thin film growth with thin seeding layers: a route to microstructural modification. Journal of Materials Chemistry C, 2015, 3, 9359-9368.	5.5	34
327	Porous carbons from inverse vulcanised polymers. Microporous and Mesoporous Materials, 2016, 232, 189-195.	4.4	34
328	Superhydrophobic and White Light-Activated Bactericidal Surface through a Simple Coating. ACS Applied Materials & Interfaces, 2017, 9, 29002-29009.	8.0	34
329	Photocatalytic and electrically conductive transparent Cl-doped ZnO thin films <i>via</i> aerosol-assisted chemical vapour deposition. Journal of Materials Chemistry A, 2018, 6, 12682-12692.	10.3	34
330	Unprecedented enhancement of wear resistance for epoxy-resin graphene composites. Nanoscale, 2021, 13, 2855-2867.	5.6	34
331	The preparation and characterization of Pt(Se3PPh)(PR3)2; the X-ray crystal structure of Pt(Se3PPh)(dppe)·CH2Cl2. Polyhedron, 1990, 9, 987-990.	2.2	33
332	Microstructural aspects of the self-propagating high temperature synthesis of hexagonal barium ferrites in an external magnetic field. Journal of Materials Chemistry, 2000, 10, 1925-1932.	6.7	33
333	The dual source APCVD of titanium nitride thin films from reaction of hexamethyldisilazane and titanium tetrachloride. Journal of Materials Chemistry, 2002, 12, 1906-1909.	6.7	33
334	Prevention of biofilm accumulation on a light-activated antimicrobial catheter material. Journal of Materials Chemistry, 2010, 20, 8668.	6.7	33
335	Group 13 β-Ketoiminate Compounds: Gallium Hydride Derivatives As Molecular Precursors to Thin Films of Ga2O3. Inorganic Chemistry, 2012, 51, 6385-6395.	4.0	33
336	Differential Phagocytosis-Based Photothermal Ablation of Inflammatory Macrophages in Atherosclerotic Disease. ACS Applied Materials & Interfaces, 2019, 11, 41009-41018.	8.0	33
337	Corrosion of One-Step Superhydrophobic Stainless-Steel Thermal Spray Coatings. ACS Applied Materials & Interfaces, 2020, 12, 1523-1532.	8.0	33
338	Highly reproducible, high-yield flow synthesis of gold nanoparticles based on a rational reactor design exploiting the reduction of passivated Au(<scp>iii</scp>). Reaction Chemistry and Engineering, 2020, 5, 663-676.	3.7	33
339	Preparation and Characterization of a Material of Composition BiP (Bismuth Phosphide) and Other Intergroup 15 Element Phases. Chemistry of Materials, 1997, 9, 1385-1392.	6.7	32
340	Aerosol-Assisted Chemical Vapor Deposition of NbS2 and TaS2 Thin Films from Pentakis(dimethylamido)metal Complexes and 2-Methylpropanethiol. European Journal of Inorganic Chemistry, 2005, 2005, 4179-4185.	2.0	32
341	A comparison of the gas sensing properties of solid state metal oxide semiconductor gas sensors produced by atmospheric pressure chemical vapour deposition and screen printing. Measurement Science and Technology, 2007, 18, 190-200.	2.6	32
342	TiO2-based transparent conducting oxides; the search for optimum electrical conductivity using a combinatorial approach. Journal of Materials Chemistry C, 2013, 1, 6335.	5.5	32

#	Article	IF	CITATIONS
343	Combinatorial aerosol assisted chemical vapour deposition of a photocatalytic mixed SnO ₂ /TiO ₂ thin film. Journal of Materials Chemistry A, 2014, 2, 5108-5116.	10.3	32
344	The use of zinc oxide nanoparticles to enhance the antibacterial properties of light-activated polydimethylsiloxane containing crystal violet. RSC Advances, 2015, 5, 8806-8813.	3.6	32
345	Solid solution nitride/carbon nanotube hybrids enhance electrocatalysis of oxygen in zinc-air batteries. Energy Storage Materials, 2018, 15, 380-387.	18.0	32
346	Sol–Gel Synthesis of Highâ€Density Zeolitic Imidazolate Framework Monoliths via Ligand Assisted Methods: Exceptional Porosity, Hydrophobicity, and Applications in Vapor Adsorption. Advanced Functional Materials, 2021, 31, 2008357.	14.9	32
347	Self-propagating routes to transition-metal phosphides. Journal of Materials Chemistry, 1994, 4, 279.	6.7	31
348	Self-propagating high-temperature synthesis of barium-chromium ferrites BaFe12-xCrxO19(Olexle6.0). Journal Physics D: Applied Physics, 1999, 32, 2590-2598.	2.8	31
349	Self-propagating high-temperature synthesis of chromium substituted lanthanum orthoferrites LaFe1 Ⱂ xCrxO3 (0 ≤ ≤). Journal of Materials Chemistry, 2001, 11, 854-858.	6.7	31
350	The gas-sensing properties of WO3â^'xthin films deposited via the atmospheric pressure chemical vapour deposition (APCVD) of WCl6with ethanol. Measurement Science and Technology, 2008, 19, 025203.	2.6	31
351	Nâ€Doped Titania Thin Films Prepared by Atmospheric Pressure CVD using <i>t</i> â€Butylamine as the Nitrogen Source: Enhanced Photocatalytic Activity under Visible Light. Chemical Vapor Deposition, 2009, 15, 171-174.	1.3	31
352	An investigation into the effect of thickness of titanium dioxide and gold–silver nanoparticle titanium dioxide composite thin-films on photocatalytic activity and photo-induced oxygen production in a sacrificial system. Journal of Materials Chemistry, 2011, 21, 6854.	6.7	31
353	Lethal photosensitisation of bacteria using a tin chlorin e6–glutathione–gold nanoparticle conjugate. Journal of Materials Chemistry, 2011, 21, 4189.	6.7	31
354	Atmospheric pressure chemical vapour deposition of boron doped titanium dioxide for photocatalytic water reduction and oxidation. Physical Chemistry Chemical Physics, 2013, 15, 16788.	2.8	31
355	Spherical β-cyclodextrin-silica hybrid materials for multifunctional chiral stationary phases. Journal of Chromatography A, 2015, 1383, 70-78.	3.7	31
356	Comparative study of singlet oxygen production by photosensitiser dyes encapsulated in silicone: towards rational design of anti-microbial surfaces. Physical Chemistry Chemical Physics, 2016, 18, 28101-28109.	2.8	31
357	Selective Detection of Nitroexplosives Using Molecular Recognition within Self-Assembled Plasmonic Nanojunctions. Journal of Physical Chemistry C, 2019, 123, 15769-15776.	3.1	31
358	Fluorine-Free Transparent Superhydrophobic Nanocomposite Coatings from Mesoporous Silica. Langmuir, 2020, 36, 13426-13438.	3.5	31
359	Delayed Lubricant Depletion of Slippery Liquid Infused Porous Surfaces Using Precision Nanostructures. Langmuir, 2021, 37, 10071-10078.	3.5	31
360	Convenient synthesis of lanthanide and mixed lanthanide phosphides by solid-state routes involving sodium phosphide. Journal of Materials Chemistry, 1993, 3, 689.	6.7	30

#	Article	IF	CITATIONS
361	Self-Propagating High Temperature Synthesis of Hexagonal Ferrites MFe12O19 (M = Sr, Ba). Advanced Materials, 1997, 9, 643-645.	21.0	30
362	Chemical vapour deposition of titanium chalcogenides and pnictides and tungsten oxide thin films. New Journal of Chemistry, 2006, 30, 505.	2.8	30
363	Quantum dots as enhancers of the efficacy of bacterial lethal photosensitization. Nanotechnology, 2008, 19, 445102.	2.6	30
364	The Effect of Solvent on the Phase of Titanium Dioxide Deposited by Aerosolâ€assisted CVD. Chemical Vapor Deposition, 2012, 18, 126-132.	1.3	30
365	The room temperature formation of gold nanoparticles from the reaction of cyclohexanone and auric acid; a transition from dendritic particles to compact shapes and nanoplates. Journal of Materials Chemistry A, 2013, 1, 7351.	10.3	30
366	Photoactivable Polymers Embedded with Cadmium-Free Quantum Dots and Crystal Violet: Efficient Bactericidal Activity against Clinical Strains of Antibiotic-Resistant Bacteria. ACS Applied Materials & Interfaces, 2019, 11, 12367-12378.	8.0	30
367	Solid state metathesis synthesis of metal silicides; reactions of calcium and magnesium silicide with metal oxides. Polyhedron, 2002, 21, 187-191.	2.2	29
368	Superhydrophobic polymer films via aerosol assisted deposition — Taking a leaf out of nature's book. Thin Solid Films, 2010, 518, 4328-4335.	1.8	29
369	The gas sensing properties of some complex metal oxides prepared by self-propagating high-temperature synthesis. Materials Letters, 2012, 75, 36-38.	2.6	29
370	On the nature of niobium substitution in niobium doped titania thin films by AACVD and its impact on electrical and optical properties. Journal of Materials Chemistry A, 2015, 3, 17755-17762.	10.3	29
371	Effect of pretreatment temperature on the photocatalytic activity of microwave irradiated porous nanocrystalline ZnO. New Journal of Chemistry, 2015, 39, 321-332.	2.8	29
372	Plasmonic Nanoprobes for Stimulated Emission Depletion Nanoscopy. ACS Nano, 2016, 10, 10454-10461.	14.6	29
373	On the apparent visible-light and enhanced UV-light photocatalytic activity of nitrogen-doped TiO 2 thin films. Journal of Photochemistry and Photobiology A: Chemistry, 2017, 333, 49-55.	3.9	29
374	High Defect Nanoscale ZnO Films with Polar Facets for Enhanced Photocatalytic Performance. ACS Applied Nano Materials, 2019, 2, 2881-2889.	5.0	29
375	Radio-metal cross-linking of alginate hydrogels for non-invasive in vivo imaging. Biomaterials, 2020, 243, 119930.	11.4	29
376	The Effect of Photoinduced Surface Oxygen Vacancies on the Charge Carrier Dynamics in TiO ₂ Films. Nano Letters, 2021, 21, 8348-8354.	9.1	29
377	Tin phosphide coatings from the atmospheric pressure chemical vapour deposition of SnX4 (X=Cl or) Tj ETQq1 1	0.784314	f rgBT /Over
378	Atmospheric pressure chemical vapour deposition of TiS2 thin films on glass. Polyhedron, 2003, 22, 1263-1269.	2.2	28

#	Article	IF	CITATIONS
379	Dual-source chemical vapour deposition of titanium sulfide thin films from tetrakisdimethylamidotitanium and sulfur precursors. Journal of Materials Chemistry, 2004, 14, 3474.	6.7	28
380	Temperature and thickness-dependent growth behaviour and opto-electronic properties of Ga-doped ZnO films prepared by aerosol-assisted chemical vapour deposition. Journal of Materials Chemistry A, 2014, 2, 17174-17182.	10.3	28
381	Organic–inorganic hybrid materials: nanoparticle containing organogels with myriad applications. Chemical Communications, 2014, 50, 14418-14420.	4.1	28
382	Photosensitisation studies of silicone polymer doped with methylene blue and nanogold for antimicrobial applications. RSC Advances, 2015, 5, 54830-54842.	3.6	28
383	Single step route to highly transparent, conductive and hazy aluminium doped zinc oxide films. RSC Advances, 2018, 8, 42300-42307.	3.6	28
384	Heterojunction αâ€Fe ₂ O ₃ /ZnO Films with Enhanced Photocatalytic Properties Grown by Aerosolâ€Assisted Chemical Vapour Deposition. Chemistry - A European Journal, 2019, 25, 11337-11345.	3.3	28
385	Reactive silica nanoparticles turn epoxy coating from hydrophilic to super-robust superhydrophobic. RSC Advances, 2019, 9, 12547-12554.	3.6	28
386	Zn and N Codoped TiO ₂ Thin Films: Photocatalytic and Bactericidal Activity. ACS Applied Materials & Interfaces, 2021, 13, 10480-10489.	8.0	28
387	Surfactant directed chemical vapour deposition of gold nanoparticles with narrow size distributions. Gold Bulletin, 2008, 41, 66-69.	2.7	27
388	Templated growth of smart coatings: Hybrid chemical vapour deposition of vanadyl acetylacetonate with tetraoctyl ammonium bromide. Applied Surface Science, 2009, 255, 7291-7295.	6.1	27
389	Efficacy of a Novel Light-Activated Antimicrobial Coating for Disinfecting Hospital Surfaces. Infection Control and Hospital Epidemiology, 2011, 32, 1130-1132.	1.8	27
390	Nanocellulose 3, 5â€Dimethylphenylcarbamate Derivative Coated Chiral Stationary Phase: Preparation and Enantioseparation Performance. Chirality, 2016, 28, 376-381.	2.6	27
391	Synthesis and material characterization ofÂamorphous and crystalline (α-) Al ₂ O ₃ via aerosol assisted chemical vapour deposition. RSC Advances, 2016, 6, 102956-102960.	3.6	27
392	Computational and Experimental Study of Ta ₂ O ₅ Thin Films. Journal of Physical Chemistry C, 2017, 121, 202-210.	3.1	27
393	A Light-Activated Antimicrobial Surface Is Active Against Bacterial, Viral and Fungal Organisms. Scientific Reports, 2017, 7, 15298.	3.3	27
394	Room Temperature Synthesis of Phosphineâ€Capped Lead Bromide Perovskite Nanocrystals without Coordinating Solvents. Particle and Particle Systems Characterization, 2020, 37, 1900391.	2.3	27
395	High Conductivity La2-xSrxCu1-y(Mg, Al)yO4Solid State Metal Oxide Gas Sensors with the K2NiF4Structure. Chemistry of Materials, 2006, 18, 3351-3355.	6.7	26
396	Transition Metal Exchanged Zeolite Layers for Selectivity Enhancement of Metal-Oxide Semiconductor Gas Sensors. IEEE Sensors Journal, 2007, 7, 551-556.	4.7	26

#	Article	IF	CITATIONS
397	Particle size, morphology and phase transitions in hydrothermally produced VO ₂ (D). New Journal of Chemistry, 2017, 41, 9216-9222.	2.8	26
398	Encapsulation of metal precursor within ZIFs for bimetallic N-doped carbon electrocatalyst with enhanced oxygen reduction. International Journal of Hydrogen Energy, 2018, 43, 14701-14709.	7.1	26
399	Inexpensive and non-toxic water repellent coatings comprising SiO ₂ nanoparticles and long chain fatty acids. RSC Advances, 2018, 8, 27064-27072.	3.6	26
400	Formation of transition-metal nitrides from the reactions of lithium amides and anhydrous transition-metal chlorides. Journal of Materials Chemistry, 1995, 5, 909.	6.7	25
401	Solid-state and solution phase metathetical synthesis of copper indium chalcogenides. Journal of Materials Chemistry, 1998, 8, 2209-2211.	6.7	25
402	Laser-induced combustion synthesis of 3D functional materials: computer-aided design. Journal of Materials Chemistry, 2004, 14, 3444.	6.7	25
403	Superhydrophobic silica films on glass formed by hydrolysis of an acidic aerosol of tetraethylorthosilicate. Journal of Materials Chemistry, 2011, 21, 9362.	6.7	25
404	Antimicrobial Properties of Light-activated Polyurethane Containing Indocyanine Green. Journal of Biomaterials Applications, 2011, 25, 387-400.	2.4	25
405	Controlling the Cross-Sensitivity of Carbon Nanotube-Based Gas Sensors to Water Using Zeolites. ACS Applied Materials & Interfaces, 2016, 8, 28096-28104.	8.0	25
406	Graphene quantum dots as additives in capillary electrophoresis for separation cinnamic acid and its derivatives. Analytical Biochemistry, 2016, 500, 38-44.	2.4	25
407	White Light-Activated Antimicrobial Paint using Crystal Violet. ACS Applied Materials & Interfaces, 2016, 8, 15033-15039.	8.0	25
408	Correlation of Optical Properties, Electronic Structure, and Photocatalytic Activity in Nanostructured Tungsten Oxide. Advanced Materials Interfaces, 2017, 4, 1700064.	3.7	25
409	Interstitial boron-doped anatase TiO ₂ thin-films on optical fibres: atmospheric pressure-plasma enhanced chemical vapour deposition as the key for functional oxide coatings on temperature-sensitive substrates. Journal of Materials Chemistry A, 2017, 5, 10836-10842.	10.3	25
410	Electronic properties of antimony-doped anatase TiO ₂ thin films prepared by aerosol assisted chemical vapour deposition. Journal of Materials Chemistry C, 2017, 5, 9694-9701.	5.5	25
411	White-Light-Activated Antibacterial Surfaces Generated by Synergy between Zinc Oxide Nanoparticles and Crystal Violet. ACS Omega, 2018, 3, 3190-3199.	3.5	25
412	Multifunctional Porous and Magnetic Silicone with High Elasticity, Durability, and Oil–Water Separation Properties. Langmuir, 2018, 34, 13305-13311.	3.5	25
413	Video-rate all-optical ultrasound imaging. Biomedical Optics Express, 2018, 9, 3481.	2.9	25
414	Elemental, liquid ammonia facilitated routes to zinc, cadmium, mercury copper, silver and lead telluride. Journal of Materials Science Letters, 1996, 15, 1741-1742.	0.5	24

#	Article	IF	CITATIONS
415	The effect of large magnetic fields on solid state combustion reactions: novel microstructure, lattice contraction and reduced coercivity in barium hexaferrite. Journal of Materials Chemistry, 2000, 10, 235-237.	6.7	24
416	Self-propagating high temperature synthesis of MFe12O19 (M=Sr,Ba) from the reactions of metal superoxides and iron metal. Journal of Materials Processing Technology, 2001, 110, 239-243.	6.3	24
417	Synthesis of a Homoleptic Niobium(V) Thiolate Complex and the Preparation of Niobium Sulfide via Thio "Solâ^'Gel―and Vapor Phase Thin-Film Experiments. Inorganic Chemistry, 2002, 41, 3668-3672.	4.0	24
418	Aerosol-assisted chemical vapour deposition of sodium fluoride thin films. Thin Solid Films, 2004, 469-470, 416-419.	1.8	24
419	Templated growth of smart nanocomposite thin films: Hybrid aerosol assisted and atmospheric pressure chemical vapour deposition of vanadyl acetylacetonate, auric acid and tetraoctyl ammonium bromide. Polyhedron, 2009, 28, 2233-2239.	2.2	24
420	A comprehensive aerosol spray method for the rapid photocatalytic grid area analysis of semiconductor photocatalyst thin films. Analytica Chimica Acta, 2010, 663, 69-76.	5.4	24
421	Gallium and Indium βâ€Diketonate Complexes: AACVD of [In(thd) ₃] and the Attempted Synthesis of Gallium and Indium Bis(βâ€diketonates). European Journal of Inorganic Chemistry, 2011, 2011, 1953-1960.	2.0	24
422	Oneâ€Pot Synthesis of Coreâ€Shell Silverâ€Gold Nanoparticle Solutions and Their Interaction with Methylene Blue Dye. European Journal of Inorganic Chemistry, 2011, 2011, 4534-4544.	2.0	24
423	Urchin-like MnO2 capped ZnO nanorods as high-rate and high-stability pseudocapacitor electrodes. Electrochimica Acta, 2015, 186, 1-6.	5.2	24
424	TiO ₂ â€coated CoCrMo: Improving the osteogenic differentiation and adhesion of mesenchymal stem cells <i>in vitro</i> . Journal of Biomedical Materials Research - Part A, 2015, 103, 1208-1217.	4.0	24
425	Chemically Treated 3D Printed Polymer Scaffolds for Biomineral Formation. ACS Omega, 2018, 3, 4342-4351.	3.5	24
426	Charge Transport Phenomena in Heterojunction Photocatalysts: The WO ₃ /TiO ₂ System as an Archetypical Model. ACS Applied Materials & Interfaces, 2021, 13, 9781-9793.	8.0	24
427	Enhancing Hydrogen Evolution Electrocatalytic Performance in Neutral Media via Nitrogen and Iron Phosphide Interactions. Small Science, 2021, 1, 2100032.	9.9	24
428	Combustion Synthesis of BaFe12O19 in an External Magnetic Field: Time-Resolved X-ray Diffraction (TRXRD) Studies. Advanced Materials, 2000, 12, 1359-1362.	21.0	23
429	Single-source CVD routes to titanium phosphide. Dalton Transactions RSC, 2002, , 2702-2709.	2.3	23
430	Molecular precursors for the CVD of niobium and tantalum nitride. Polyhedron, 2005, 24, 463-468.	2.2	23
431	Magnetic hyperthermia controlled drug release in the GI tract: solving the problem of detection. Scientific Reports, 2016, 6, 34271.	3.3	23
432	InGaN/GaN Multiple Quantum Well Photoanode Modified with Cobalt Oxide for Water Oxidation. ACS Applied Energy Materials, 2018, 1, 6417-6424.	5.1	23

#	Article	IF	CITATIONS
433	Optimization of the thermochromic glazing design for curtain wall buildings based on experimental measurements and dynamic simulation. Solar Energy, 2021, 216, 14-25.	6.1	23
434	Self-propagating high temperature synthesis of BaFe12O19, Mg0.5Zn0.5Fe2O4 and Li0.5Fe2.5O4; time resolved X-ray diffraction studies (TRXRD). Journal of Materials Chemistry, 2001, 11, 193-199.	6.7	22
435	Atmospheric pressure chemical vapour deposition of Cr2â^'xTixO3(CTO) thin films (â‰ \$ µm) on to gas sensing substrates. Journal of Materials Chemistry, 2003, 13, 2957-2962.	6.7	22
436	Ultra-violet light activated photocatalysis in thin films of the titanium oxynitride, Ti3â^ÎO4N. Journal of Photochemistry and Photobiology A: Chemistry, 2009, 203, 199-203.	3.9	22
437	The use of combinatorial aerosol-assisted chemical vapour deposition for the formation of gallium-indium-oxide thin films. Journal of Materials Chemistry, 2011, 21, 12644.	6.7	22
438	Gas Sensing Studies of a n-n Hetero-Junction Array Based on WO ₃ and ZnO Composites. IEEE Sensors Journal, 2014, 14, 3137-3147.	4.7	22
439	Synthesis and characterisation of novel aluminium and gallium precursors for chemical vapour deposition. New Journal of Chemistry, 2015, 39, 6585-6592.	2.8	22
440	The bactericidal activity of glutaraldehydeâ€impregnated polyurethane. MicrobiologyOpen, 2016, 5, 891-897.	3.0	22
441	A Targeted Functional Design for Highly Efficient and Stable Cathodes for Rechargeable Liâ€ion Batteries. Advanced Functional Materials, 2017, 27, 1604903.	14.9	22
442	Qualitative XANES and XPS Analysis of Substrate Effects in VO ₂ Thin Films: A Route to Improving Chemical Vapor Deposition Synthetic Methods?. Journal of Physical Chemistry C, 2017, 121, 20345-20352.	3.1	22
443	Flexible and Strong Robust Superhydrophobic Monoliths with Antibacterial Property. ACS Applied Polymer Materials, 2020, 2, 4856-4863.	4.4	22
444	Antimicrobial surfaces: A need for stewardship?. PLoS Pathogens, 2020, 16, e1008880.	4.7	22
445	High-Performance Planar Thin Film Thermochromic Window via Dynamic Optical Impedance Matching. ACS Applied Materials & Interfaces, 2020, 12, 8140-8145.	8.0	22
446	A coating-free superhydrophobic sensing material for full-range human motion and microliter droplet impact detection. Chemical Engineering Journal, 2021, 410, 128418.	12.7	22
447	Probing the Role of Atomic Defects in Photocatalytic Systems through Photoinduced Enhanced Raman Scattering. ACS Energy Letters, 2021, 6, 4273-4281.	17.4	22
448	Platinum Complexes of the Anions Se2N22? and Se2N2H?; X-Ray Structure Analysis of [Pt(Se2N2H) (PMe2Ph)2]Cl. Angewandte Chemie International Edition in English, 1989, 28, 1047-1049.	4.4	21
449	Preparation and ligand properties of bis-thionylimino complexes of the type M(NSO)2(PR3)2. X-ray structure of Pt(NSO)2(PMe3)2. Polyhedron, 1989, 8, 835-839.	2.2	21
450	Tungsten(6+) Tris(pinacolate): Structure and Comments on the Preference for an Octahedral Geometry Relative to Trigonal Prismatic (D3h) for a d0 Complex in the Presence of Strong .piDonor Ligands. Inorganic Chemistry, 1994, 33, 812-815.	4.0	21

#	Article	IF	CITATIONS
451	Convenient, low energy routes to hexagonal ferrites MFe12O19(M=Sr, Ba) from SHS reactions of iron, iron oxide and MO2 in air. Journal of Materials Chemistry, 1998, 8, 573-578.	6.7	21
452	Combustion synthesis of chromium-substituted lithium ferrites Li0.5Fe2.5â^'xCrxO4 (xâ‰ 2 .0): Rietveld analysis and magnetic measurements. Solid State Sciences, 1999, 1, 311-316.	0.7	21
453	Sodium borohydride reduction of aqueous iron–zirconium solutions: chemical routes to amorphous and nanocrystalline Fe–Zr–B alloys. Journal of Materials Chemistry, 1999, 9, 2537-2544.	6.7	21
454	Combustion synthesis of alkaline-earth substituted lanthanum manganites; LaMnO3, La0.6Ca0.4MnO3 and La0.6Sr0.4MnO3. Journal of Materials Chemistry, 2004, 14, 1377.	6.7	21
455	Dual source APCVD synthesis of TaN and NbN thin films on glass from the reaction of MCl5 (M = Ta,) Tj ETQq1 1	0.784314 6.7	rgBT /Over
456	Self propagating high temperature synthesis of magnesium zinc ferrites (MgxZn1 â^ xFe2O3): thermal imaging and time resolved X-ray diffraction experiments. Journal of Materials Chemistry, 2004, 14, 1104-1111.	6.7	21
457	Surface Laser Sintering of exothermic powder compositions. Journal of Thermal Analysis and Calorimetry, 2008, 91, 427-436.	3.6	21
458	Aerosolâ€Assisted Chemical Vapour Deposition of a Copper Gallium Oxide Spinel. ChemPlusChem, 2014, 79, 122-127.	2.8	21
459	The antibacterial properties of light-activated polydimethylsiloxane containing crystal violet. RSC Advances, 2014, 4, 51711-51715.	3.6	21
460	Suspension plasma sprayed coatings using dilute hydrothermally produced titania feedstocks for photocatalytic applications. Journal of Materials Chemistry A, 2015, 3, 12680-12689.	10.3	21
461	Light-activated antibacterial screen protectors for mobile telephones and tablet computers. Journal of Photochemistry and Photobiology A: Chemistry, 2015, 296, 19-24.	3.9	21
462	High-Throughput Synthesis, Screening, and Scale-Up of Optimized Conducting Indium Tin Oxides. ACS Combinatorial Science, 2016, 18, 130-137.	3.8	21
463	Antibacterial Surfaces with Activity against Antimicrobial Resistant Bacterial Pathogens and Endospores. ACS Infectious Diseases, 2020, 6, 939-946.	3.8	21
464	Electron-Deficient Au Nanoparticles Confined in Organic Molecular Cages for Catalytic Reduction of 4-Nitrophenol. ACS Applied Nano Materials, 2022, 5, 1276-1283.	5.0	21
465	Self-propagating high temperature synthesis of yttrium iron chromium garnets Y3Fe5 â^' xCrxO12 (0 ≤) Tj ET	Qq1_1 0.7 6.7	784314 rgB 20
466	Titanium Phosphide Coatings from the Atmospheric Pressure Chemical Vapor Deposition of TiCl4and RPH2(R =t-Bu, Ph, CyHex). Chemistry of Materials, 2002, 14, 3167-3173.	6.7	20
467	Composite thermochromic thin films: (TiO2)–(VO2) prepared from titanium isopropoxide, VOCl3 and water. Polyhedron, 2006, 25, 334-338.	2.2	20
468	Antimony oxide thin films from the atmospheric pressure chemical vapour deposition reaction of antimony pentachloride and ethyl acetate. Polyhedron, 2006, 25, 3032-3038.	2.2	20

#	Article	IF	CITATIONS
469	Synthetic and Structural Studies of Donor-Functionalized Alkoxy Derivatives of Gallium. Inorganic Chemistry, 2011, 50, 9491-9498.	4.0	20
470	Study of the adhesion of Staphylococcus aureus to coated glass substrates. Journal of Materials Science, 2011, 46, 6355-6363.	3.7	20
471	Callium Hydride Complexes Stabilised by Multidentate Alkoxide Ligands: Precursors to Thin Films of Ga ₂ O ₃ at Low Temperatures. Chemistry - A European Journal, 2012, 18, 6079-6087.	3.3	20
472	A fast and effective method for N-doping TiO2 by post treatment with liquid ammonia: visible light photocatalysis. Thin Solid Films, 2014, 562, 223-228.	1.8	20
473	Prolonging the circulatory retention of SPIONs using dextran sulfate: in vivo tracking achieved by functionalisation with near-infrared dyes. Faraday Discussions, 2014, 175, 41-58.	3.2	20
474	Nanocellulose crystals derivative-silica hybrid sol open tubular capillary column for enantioseparation. Carbohydrate Polymers, 2017, 165, 359-367.	10.2	20
475	Nanoscale, conformal films of graphitic carbon nitride deposited at room temperature: a method for construction of heterojunction devices. Nanoscale, 2017, 9, 16586-16590.	5.6	20
476	Nb-doped rutile titanium dioxide nanorods for lithium-ion batteries. Solid State Sciences, 2018, 83, 115-121.	3.2	20
477	Origin of High-Efficiency Photoelectrochemical Water Splitting on Hematite/Functional Nanohybrid Metal Oxide Overlayer Photoanode after a Low Temperature Inert Gas Annealing Treatment. ACS Omega, 2019, 4, 1449-1459.	3.5	20
478	Nanostructured titanium dioxide coatings prepared by Aerosol Assisted Chemical Vapour Deposition (AACVD). Journal of Photochemistry and Photobiology A: Chemistry, 2020, 400, 112727.	3.9	20
479	Thio sol–gel synthesis of titanium disulfide from titanium thiolates. Journal of Materials Chemistry, 2000, 10, 2823-2826.	6.7	19
480	Atmospheric-Pressure Chemical Vapor Deposition of Group IVb Metal Phosphide Thin Films from Tetrakisdimethylamidometal Complexes and Cyclohexylphosphine. Chemistry of Materials, 2004, 16, 1120-1125.	6.7	19
481	Photocatalytic evolution of hydrogen and oxygen from ceramic wafers of commercial titanias. Journal of Photochemistry and Photobiology A: Chemistry, 2010, 216, 110-114.	3.9	19
482	Relationship between surface hydrophobicity and water bounces – a dynamic method for accessing surface hydrophobicity. Journal of Materials Chemistry A, 2013, 1, 799-804.	10.3	19
483	A simple and low-cost method for the preparation of self-supported TiO ₂ –WO ₃ ceramic heterojunction wafers. Journal of Materials Chemistry A, 2014, 2, 17602-17608.	10.3	19
484	Doping Group IIB Metal Ions into Quantum Dot Shells via the Oneâ€Pot Decomposition of Metalâ€Dithiocarbamates. Advanced Optical Materials, 2015, 3, 704-712.	7.3	19
485	Aerosol assisted chemical vapour deposition of a ZrO ₂ –TiO ₂ composite thin film with enhanced photocatalytic activity. RSC Advances, 2015, 5, 67944-67950.	3.6	19
486	Functional thin film coatings incorporating gold nanoparticles in a transparent conducting fluorine doped tin oxide matrix. Journal of Materials Chemistry C, 2015, 3, 1118-1125.	5.5	19

#	Article	IF	CITATIONS
487	A single-source precursor approach to solution processed indium arsenide thin films. Journal of Materials Chemistry C, 2016, 4, 6761-6768.	5.5	19
488	A SPION-eicosane protective coating for water soluble capsules: Evidence for on-demand drug release triggered by magnetic hyperthermia. Scientific Reports, 2016, 6, 20271.	3.3	19
489	White light-activated antimicrobial surfaces: effect of nanoparticles type on activity. Journal of Materials Chemistry B, 2016, 4, 2199-2207.	5.8	19
490	Superoleophobic surfaces on stainless steel substrates obtained by chemical bath deposition. Micro and Nano Letters, 2017, 12, 76-81.	1.3	19
491	Computational Intelligenceâ€Assisted Understanding of Natureâ€Inspired Superhydrophobic Behavior. Advanced Science, 2018, 5, 1700520.	11.2	19
492	Heteroepitaxy of GaP on silicon for efficient and cost-effective photoelectrochemical water splitting. Journal of Materials Chemistry A, 2019, 7, 8550-8558.	10.3	19
493	Nonmonotonic contactless manipulation of binary droplets via sensing of localized vapor sources on pristine substrates. Science Advances, 2020, 6, .	10.3	19
494	Dual source atmospheric pressure chemical vapour deposition of TiP films on glass using TiCl4 and PH2But. Journal of Materials Chemistry, 2001, 11, 2408-2409.	6.7	18
495	Thiolate derivatives of titanium(iv) and tantalum(v) as precursors to metal sulfides. Dalton Transactions RSC, 2001, , 2554-2558.	2.3	18
496	Self-propagating solid state routes to BaSnO3; investigation of gas sensing properties. Journal of Materials Science, 2002, 37, 375-379.	3.7	18
497	Photocatalytic Oxidation of Deposited Sulfur and Gaseous Sulfur Dioxide by TiO2 Films. Journal of Physical Chemistry C, 2007, 111, 5520-5525.	3.1	18
498	Nanoparticulate cerium dioxide and cerium dioxide–titanium dioxide composite thin films on glass by aerosol assisted chemical vapour deposition. Applied Surface Science, 2009, 256, 852-856.	6.1	18
499	An Investigation into the Optimum Thickness of Titanium Dioxide Thin Films Synthesized by Using Atmospheric Pressure Chemical Vapour Deposition for Use in Photocatalytic Water Oxidation. Chemistry - A European Journal, 2010, 16, 10546-10552.	3.3	18
500	Aerosol assisted deposition of melamine-formaldehyde resin: Hydrophobic thin films from a hydrophilic material. Thin Solid Films, 2011, 519, 2181-2186.	1.8	18
501	Enhanced Bactericidal Activity of Silver Thin Films Deposited via Aerosol-Assisted Chemical Vapor Deposition. ACS Applied Materials & Interfaces, 2015, 7, 28616-28623.	8.0	18
502	Gas Sensing Studies of an n-n Hetero-Junction Array Based on SnO2 and ZnO Composites. Chemosensors, 2016, 4, 3.	3.6	18
503	Fabrication of Long-Term Underwater Superoleophobic Al Surfaces and Application on Underwater Lossless Manipulation of Non-Polar Organic Liquids. Scientific Reports, 2016, 6, 31818.	3.3	18
504	Photo-activity and low resistivity in N/Nb Co-doped TiO ₂ thin films by combinatorial AACVD. Journal of Materials Chemistry A, 2016, 4, 407-415.	10.3	18

#	Article	IF	CITATIONS
505	Ultraviolet Radiation Induced Dopant Loss in a TiO ₂ Photocatalyst. ACS Catalysis, 2017, 7, 1485-1490.	11.2	18
506	Continuous separation of maslinic and oleanolic acids from olive pulp by highâ€speed countercurrent chromatography with elutionâ€extrusion mode. Journal of Separation Science, 2019, 42, 2080-2088.	2.5	18
507	Rapid synthesis of [Au25(Cys)18] nanoclusters via carbon monoxide in microfluidic liquid-liquid segmented flow system and their antimicrobial performance. Chemical Engineering Journal, 2020, 383, 123176.	12.7	18
508	N ₂ Electroreduction to NH ₃ by Selenium Vacancyâ€Rich ReSe ₂ Catalysis at an Abrupt Interface. Angewandte Chemie, 2020, 132, 13422-13429.	2.0	18
509	A convenient low temperature route to the formation of lanthanide oxides. Inorganica Chimica Acta, 1993, 211, 77-80.	2.4	17
510	Liquid Ammonia Mediated Metathesis:Â Synthesis of Binary Metal Chalcogenides and Pnictides. Inorganic Chemistry, 2001, 40, 6940-6947.	4.0	17
511	Tungsten Oxide and Tungsten Oxide-Titania Thin Films Prepared by Aerosol-Assisted Deposition – Use of Preformed Solid Nanoparticles. European Journal of Inorganic Chemistry, 2007, 2007, 1415-1421.	2.0	17
512	Frictional properties of light-activated antimicrobial polymers in blood vessels. Journal of Materials Science: Materials in Medicine, 2010, 21, 815-821.	3.6	17
513	Halide doping effects on transparent conducting oxides formed by aerosol assisted chemical vapour deposition. Thin Solid Films, 2013, 532, 26-30.	1.8	17
514	Silver enhanced TiO ₂ thin films: photocatalytic characterization using aqueous solutions of tris(hydroxymethyl)aminomethane. Dalton Transactions, 2014, 43, 344-351.	3.3	17
515	Aerosolâ€Assisted Chemicalâ€Vapour Deposition of Zinc Oxide from Singleâ€Source βâ€Iminoesterate Precursors. European Journal of Inorganic Chemistry, 2015, 2015, 3658-3665.	2.0	17
516	Incorporation of crystal violet, methylene blue and safranin O into a copolymer emulsion; the development of a novel antimicrobial paint. RSC Advances, 2015, 5, 26364-26375.	3.6	17
517	Synthesis and characterization of omniphobic surfaces with thermal, mechanical and chemical stability. RSC Advances, 2016, 6, 106491-106499.	3.6	17
518	High-Throughput Continuous Hydrothermal Synthesis of Transparent Conducting Aluminum and Gallium Co-doped Zinc Oxides. ACS Combinatorial Science, 2017, 19, 239-245.	3.8	17
519	Synthesis of superhydrophobic surfaces with Wenzel and Cassie–Baxter state: experimental evidence and theoretical insight. Nanotechnology, 2018, 29, 485601.	2.6	17
520	Dispelling the Myth of Passivated Codoping in TiO ₂ . Chemistry of Materials, 2019, 31, 2577-2589.	6.7	17
521	Self propagating high temperature synthesis of BaFe12â^'xCrxO19 and Li0.5Fe2.5â^'xCrxO4. Journal of Materials Chemistry, 1999, 9, 273-281.	6.7	16
522	Synthesis and Characterization of a Homoleptic Thiolate Complex of Titanium(IV). Inorganic Chemistry, 2000, 39, 2693-2695.	4.0	16

#	Article	IF	CITATIONS
523	Solid state synthesis of binary metal chalcogenides. Dalton Transactions RSC, 2001, , 1872-1875.	2.3	16
524	Structural distortions in homoleptic (RE)4A (E = O, S, Se; A = C, Si, Ge, Sn): implications for the CVD of tin sulfides. Dalton Transactions RSC, 2001, , 3435-3445.	2.3	16
525	Chemical vapour deposition of group Vb metal phosphide thin films. Journal of Materials Chemistry, 2003, 13, 1930.	6.7	16
526	The effect of oxygen-containing reagents on the crystal morphology and orientation in tungsten oxide thin films deposited via atmospheric pressure chemical vapour deposition (APCVD) on glass substrates. Faraday Discussions, 2007, 136, 329.	3.2	16
527	Antimicrobial Activity in Thin Films of Pseudobrookiteâ€Structured Titanium Oxynitride under UV Irradiation Observed for <i>Escherichia coli</i> . Chemical Vapor Deposition, 2010, 16, 19-22.	1.3	16
528	Selfâ€Assembled Ultraâ€High Aspect Ratio Silver Nanochains. Advanced Materials, 2012, 24, 5227-5235.	21.0	16
529	An EXAFS study on the photo-assisted growth of silver nanoparticles on titanium dioxide thin-films and the identification of their photochromic states. Physical Chemistry Chemical Physics, 2013, 15, 8254.	2.8	16
530	Functionalised gold and titania nanoparticles and surfaces for use as antimicrobial coatings. Faraday Discussions, 2014, 175, 273-287.	3.2	16
531	Advanced analysis of nanoparticle composites – a means toward increasing the efficiency of functional materials. RSC Advances, 2015, 5, 53789-53795.	3.6	16
532	Fabrication of optimized oil–water separation devices through the targeted treatment of silica meshes. Science and Technology of Advanced Materials, 2015, 16, 055006.	6.1	16
533	Power-free water pump based on a superhydrophobic surface: generation of a mushroom-like jet and anti-gravity long-distance transport. Journal of Materials Chemistry A, 2016, 4, 13771-13777.	10.3	16
534	Deeper Understanding of Interstitial Boron-Doped Anatase Thin Films as A Multifunctional Layer Through Theory and Experiment. Journal of Physical Chemistry C, 2018, 122, 714-726.	3.1	16
535	New Insight into the Role of Electron Transfer to O ₂ in Photocatalytic Oxidations of Acetone over TiO ₂ and the Effect of Au Cocatalyst. Journal of Physical Chemistry C, 2019, 123, 30958-30971.	3.1	16
536	Dual-triggered nanoaggregates of cucurbit[7]uril and gold nanoparticles for multi-spectroscopic quantification of creatinine in urinalysis. Journal of Materials Chemistry C, 2020, 8, 7051-7058.	5.5	16
537	Bridging amido complexes from reactions in liquid ammonia. X-ray crystal structure of [Pt(PMe2Ph)2(μ-NH2)2Pt(PMe2Ph)2](BF4)2. Polyhedron, 1989, 8, 1979-1981.	2.2	15
538	The preparation and X-ray structures of Pt(SeSN2)(PMe2Ph)2 and [Pt(SeSN2H)(PMe2Ph)2]BF4. Polyhedron, 1989, 8, 2215-2217.	2.2	15
539	New metal–sulphur–nitrogen compounds from reactions in liquid ammonia. The X-ray structures of trans-bis(acetophenone dimethylhydrazone-Nα)dichloropalladium(II) and [di(azathien)-1-yl-S1N4][2-(hydrazonoethyl)phenyl]palladium(II). Journal of the Chemical Society Dalton Transactions. 1989 1179-1185.	1.1	15
540	Preparation and properties of [M{S2N3(SO2NH2)}(PR3)2] and [Pt{SO2(NH)2}(PR3)2] from reactions in liquid ammonia. Journal of the Chemical Society Dalton Transactions, 1990, , 519.	1.1	15

#	Article	IF	CITATIONS
541	Diolates of dimolybdenum and ditungsten (MM) with seven-, eight- and nine-membered rings. Journal of the Chemical Society Chemical Communications, 1991, , 1673-1675.	2.0	15
542	Convenient, low energy, solid–liquid metathesis reactions; synthesis of TiN, TiO2, VN, VO2and TixVyN (x+y= 1). Journal of the Chemical Society Chemical Communications, 1993, .	2.0	15
543	Liquid-mediated metathetical synthesis of binary and ternary transition-metal pnictides. Polyhedron, 2000, 19, 829-833.	2.2	15
544	The reaction of GeCl4 with primary and secondary phosphines. Dalton Transactions, 2004, , 470.	3.3	15
545	Synthesis and characterisation of titanium pyridine- and pyrimidine-thiolates and their application as precursors to titanium disulfide. Polyhedron, 2007, 26, 43-48.	2.2	15
546	Chromium oxyselenide solid solutions from the atmospheric pressure chemical vapour deposition of chromyl chloride and diethylselenide. Journal of Materials Chemistry, 2008, 18, 1667.	6.7	15
547	Design of Three-Dimensional Functional Articles via Layer-by-Layer Laser Sintering of Exothermic Powder Mixtures. Materials and Manufacturing Processes, 2008, 23, 571-578.	4.7	15
548	Atmospheric Pressure Chemical Vapour Deposition of TiCl ₄ and <i>t</i> BuAsH ₂ to Form Titanium Arsenide Thin Films. European Journal of Inorganic Chemistry, 2010, 2010, 5629-5634.	2.0	15
549	Facile approach for preparation of stable water-repellent nanoparticle coating. Applied Surface Science, 2012, 258, 7907-7911.	6.1	15
550	Production of Predominantly Anatase Thin Films on Various Grades of Steel and Other Metallic Substrates From TiCl ₄ and Ethyl Acetate by Atmospheric Pressure CVD. Chemical Vapor Deposition, 2012, 18, 133-139.	1.3	15
551	Silver loaded WO3â^'x/TiO2 composite multifunctional thin films. Thin Solid Films, 2012, 520, 5516-5520.	1.8	15
552	Air purification by heterogeneous photocatalytic oxidation with multi-doped thin film titanium dioxide. Thin Solid Films, 2013, 537, 131-136.	1.8	15
553	Aerosol-assisted deposition of gold nanoparticle-tin dioxide composite films. RSC Advances, 2014, 4, 13182-13190.	3.6	15
554	Enhanced gas sensing performance of indium doped zinc oxide nanopowders. RSC Advances, 2015, 5, 85767-85774.	3.6	15
555	Reactivity of vanadium oxytrichloride with \hat{l}^2 -diketones and diesters as precursors for vanadium nitride and carbide. Materials and Design, 2016, 108, 780-790.	7.0	15
556	SWCNT photocathodes sensitised with InP/ZnS core–shell nanocrystals. Journal of Materials Chemistry C, 2016, 4, 3379-3384.	5.5	15
557	On-demand, magnetic hyperthermia-triggered drug delivery: optimisation for the GI tract. Journal of Materials Chemistry B, 2016, 4, 1704-1711.	5.8	15
558	Direct and continuous hydrothermal flow synthesis of thermochromic phase pure monoclinic VO ₂ nanoparticles. Journal of Materials Chemistry C, 2018, 6, 11731-11739.	5.5	15

#	Article	IF	CITATIONS
559	Surface radio-mineralisation mediates chelate-free radiolabelling of iron oxide nanoparticles. Chemical Science, 2019, 10, 2592-2597.	7.4	15
560	Functionalised iron oxide nanoparticles for multimodal optoacoustic and magnetic resonance imaging. Journal of Materials Chemistry B, 2019, 7, 2212-2219.	5.8	15
561	Controlling the Thermoelectric Properties of Organometallic Coordination Polymers via Ligand Design. Advanced Functional Materials, 2020, 30, 2003106.	14.9	15
562	SERS multiplexing of methylxanthine drug isomers <i>via</i> host–guest size matching and machine learning. Journal of Materials Chemistry C, 2021, 9, 12624-12632.	5.5	15
563	The preparation and x-ray characterisation of [(PPh2Me)2Pt(μ-PPhH)2Pt(PPh2Me)2] [Cl]4·CH2Cl2 and [(PPh2Me)2Pt(μ-PPhH)Pt(PPh2Me)2] [Cl]2 [PhPO2OH]2 [PhPO(OH)2]2. Inorganica Chimica Acta, 1990, 172, 159-163.	2.4	14
564	Transition Metal Pnictide Synthesis: Self Propagating Reactions Involving Sodium Arsenide, Antimonide and Bismuthide. Zeitschrift Fur Naturforschung - Section B Journal of Chemical Sciences, 1994, 49, 477-482.	0.7	14
565	Metathesis routes to lanthanide pnictides. Journal of Materials Chemistry, 1994, 4, 285.	6.7	14
566	Solid state metathesis routes to metal nitrides; use of strontium and barium nitrides as reagents and dilution effects. Polyhedron, 1997, 16, 3635-3640.	2.2	14
567	Atmospheric Pressure CVD of SnS and SnS ₂ on Glass. Chemical Vapor Deposition, 1998, 4, 222-225.	1.3	14
568	A combinatorial approach to phase synthesis and characterisation in atmospheric pressure chemical vapour deposition. Surface and Coatings Technology, 2007, 201, 8966-8970.	4.8	14
569	Rapid synthesis of gold nanostructures with cyclic and linear ketones. RSC Advances, 2013, 3, 21919.	3.6	14
570	Visible Light Photocatalytic Activity in AACVDâ€Prepared Nâ€modified TiO ₂ Thin Films. Chemical Vapor Deposition, 2014, 20, 91-97.	1.3	14
571	Conducting Al and Ga-doped zinc oxides; rapid optimisation and scale-up. Journal of Materials Chemistry A, 2016, 4, 12774-12780.	10.3	14
572	Scalable Production of Thermochromic Nb-Doped VO ₂ Nanomaterials Using Continuous Hydrothermal Flow Synthesis. Journal of Nanoscience and Nanotechnology, 2016, 16, 10104-10111.	0.9	14
573	Nanoparticles in explosives detection – the state-of-the-art and future directions. Forensic Science, Medicine, and Pathology, 2017, 13, 490-494.	1.4	14
574	Integration of supercapacitors into printed circuit boards. Journal of Energy Storage, 2018, 19, 28-34.	8.1	14
575	Super-robust superamphiphobic surface with anti-icing property. RSC Advances, 2019, 9, 27702-27709.	3.6	14
576	A rugged, self-sterilizing antimicrobial copper coating on ultra-high molecular weight polyethylene: a preliminary study on the feasibility of an antimicrobial prosthetic joint material. Journal of Materials Chemistry B, 2019, 7, 3310-3318.	5.8	14

#	Article	IF	CITATIONS
577	Photoelectrochemical water oxidation of GaP _{1â^'x} Sb _x with a direct band gap of 1.65 eV for full spectrum solar energy harvesting. Sustainable Energy and Fuels, 2019, 3, 1720-1729.	4.9	14
578	The reactions of sulphur–nitrogen species in liquid ammonia. Journal of the Chemical Society Chemical Communications, 1988, , 1479-1480.	2.0	13
579	Preparation and characterization of M2(SeAr′)6 and mixed ligand M2(OR)2(SeAr′)4 species (M = Mo, W). Polyhedron, 1990, 9, 2941-2952.	2.2	13
580	SYNTHESIS OF METAL SILICIDE POWDERS BY THERMOLYSIS OF METAL CHLORIDES WITH MAGNESIUM SILICIDE. Phosphorus, Sulfur and Silicon and the Related Elements, 1995, 101, 47-55.	1.6	13
581	New routes in the self-propagating high-temperature synthesis of barium titanium oxide. Polyhedron, 1996, 15, 1349-1353.	2.2	13
582	Self-propagating high-temperature synthesis of SrTiO3 and SrxBayTiO3 (x+y=1). Journal of Materials Science, 1996, 31, 5033-5037.	3.7	13
583	Self propagating high-temperature synthesis of chromium substituted magnesium zinc ferrites Mg0.5Zn0.5Fe2â^xCrxO4 (0â‰ ¤ â‰ ¤ .5). Journal of Materials Chemistry, 1998, 8, 2701-2706.	6.7	13
584	Superhydrophobic silica wool—a facile route to separating oil and hydrophobic solvents from water. Science and Technology of Advanced Materials, 2014, 15, 065003.	6.1	13
585	Lithiated MoO ₂ Nanorods with Greatly Improved Electrochemical Performance for Lithium Ion Batteries. European Journal of Inorganic Chemistry, 2014, 2014, 352-356.	2.0	13
586	Environmental sensing semiconducting nanoceramics made using a continuous hydrothermal synthesis pilot plant. Sensors and Actuators B: Chemical, 2015, 217, 136-145.	7.8	13
587	The <i>in situ</i> synthesis of PbS nanocrystals from lead(II) <i>n</i> -octylxanthate within a 1,3-diisopropenylbenzene–bisphenol A dimethacrylate sulfur copolymer. Royal Society Open Science, 2017, 4, 170383.	2.4	13
588	Gaseous Photocatalytic Oxidation of Formic Acid over TiO ₂ : A Comparison between the Charge Carrier Transfer and Light-Assisted Mars–van Krevelen Pathways. Journal of Physical Chemistry C, 2019, 123, 22261-22272.	3.1	13
589	Bioinspired Multifunctional Glass Surfaces through Regenerative Secondary Mask Lithography. Advanced Materials, 2021, 33, e2102175.	21.0	13
590	CuInS ₂ Quantum Dot and Polydimethylsiloxane Nanocomposites for Allâ€Optical Ultrasound and Photoacoustic Imaging. Advanced Materials Interfaces, 2021, 8, 2100518.	3.7	13
591	Kinetics-based design of a flow platform for highly reproducible on demand synthesis of gold nanoparticles with controlled size between 50 and 150Ânm and their application in SERS and PIERS sensing. Chemical Engineering Journal, 2021, 423, 129069.	12.7	13
592	Nitrogen-14 nuclear magnetic resonance studies on sulphur–nitrogen compounds. Journal of the Chemical Society Dalton Transactions, 1990, , 511-517.	1.1	12
593	REACTION OF Pt(Se2N2)(DPPE) WITH HALOGENS: A NEW ROUTE TO Se4N4. THE X-RAY CRYSTAL STRUCTURE OF 3[PtI2(DPPE)]·I2·2[CH2C2]. Phosphorus, Sulfur and Silicon and the Related Elements, 1991, 57, 273-277.	1.6	12
594	Low temperature deposition of crystalline chromium phosphide films using dual-source atmospheric pressure chemical vapour deposition. Applied Surface Science, 2004, 233, 24-28.	6.1	12

#	Article	IF	CITATIONS
595	An Investigation of Titaniumâ€Vanadium Nitride Phase Space, Conducted Using Combinatorial Atmospheric Pressure CVD. Chemical Vapor Deposition, 2008, 14, 309-312.	1.3	12
596	Syntheses, X-ray structures and CVD of titanium(iv) arsine complexes. Dalton Transactions, 2010, 39, 5325.	3.3	12
597	Combinatorial Atmospheric Pressure CVD of a Composite TiO ₂ /SnO ₂ Thin Film. Chemical Vapor Deposition, 2014, 20, 69-79.	1.3	12
598	Polydimethylsiloxane coated glass frits for low-cost and reusable water–organic solvent separation. Chemical Communications, 2014, 50, 12656-12658.	4.1	12
599	A low cost synthesis method for functionalised iron oxide nanoparticles for magnetic hyperthermia from readily available materials. Faraday Discussions, 2014, 175, 83-95.	3.2	12
600	Antibacterial properties of Cu–ZrO2thin films prepared via aerosol assisted chemical vapour deposition. Journal of Materials Chemistry B, 2016, 4, 666-671.	5.8	12
601	One-step constrained-volume synthesis of silver decorated polymer colloids with antimicrobial and sensing properties. Colloid and Polymer Science, 2017, 295, 521-527.	2.1	12
602	A free-standing porous silicon-type gel sponge with superhydrophobicity and oleophobicity. RSC Advances, 2017, 7, 31-36.	3.6	12
603	Modifying Epoxy Resins to Resist Both Fire and Water. Langmuir, 2019, 35, 14332-14338.	3.5	12
604	Application of levitation-jet synthesized nickel-based nanoparticles for gas sensing. Materials Science and Engineering B: Solid-State Materials for Advanced Technology, 2019, 244, 81-92.	3.5	12
605	Aerosol-assisted route to low-E transparent conductive gallium-doped zinc oxide coatings from pre-organized and halogen-free precursor. Chemical Science, 2020, 11, 4980-4990.	7.4	12
606	Robust Protection of Ill–V Nanowires in Water Splitting by a Thin Compact TiO ₂ Layer. ACS Applied Materials & Interfaces, 2021, 13, 30950-30958.	8.0	12
607	Magnetic Field-Induced Orientation of Modified Boron Nitride Nanosheets in Epoxy Resin with Improved Flame and Wear Resistance. Langmuir, 2021, 37, 8222-8231.	3.5	12
608	Crystal Violet-Impregnated Slippery Surface to Prevent Bacterial Contamination of Surfaces. ACS Applied Materials & Interfaces, 2021, 13, 5478-5485.	8.0	12
609	Synthesis and characterization of M2(EPh3)2(NMe2)4 compounds (E = C, Si, Ge, Sn; M = Mo, W). Polyhedron, 1993, 12, 961-965.	2.2	11
610	A synthesis of bismuth(III) phosphide: the first binary phosphide of bismuth. Journal of the Chemical Society Chemical Communications, 1994, , 1987.	2.0	11
611	Fast Metathesis Routes to Tungsten and Molybdenum Carbides. , 1999, 18, 267-268.		11
612	Combined combustion sol-gel synthesis of LiNbO3, LiTaO3, NaNbO3 and NaTaO3. Journal of Materials Science Letters, 2001, 20, 57-58.	0.5	11

#	Article	IF	CITATIONS
613	Heterogeneous combustion in electrical and magnetic fields: modification of combustion parameters and products. Physical Chemistry Chemical Physics, 2003, 5, 2291-2296.	2.8	11
614	NbS2 thin films by atmospheric pressure chemical vapour deposition and the formation of a new 1T polytype. Thin Solid Films, 2004, 469-470, 495-499.	1.8	11
615	Advanced Ways and Experimental Methods in Self-Propagating High-Temperature Synthesis (SHS) of Inorganic Materials. Materials Science Forum, 2006, 518, 181-188.	0.3	11
616	Aerosolâ€Assisted Chemical Vapour Deposition of Transparent Zinc Gallate Films. ChemPlusChem, 2014, 79, 1024-1029.	2.8	11
617	Enhancing the Magnetic Heating Capacity of Iron Oxide Nanoparticles through Their Postproduction Incorporation into Iron Oxide–Gold Nanocomposites. European Journal of Inorganic Chemistry, 2017, 2017, 2386-2395.	2.0	11
618	Elucidating iron doping induced n- to p- characteristics of Strontium titanate based ethanol sensors. Current Applied Physics, 2018, 18, 246-253.	2.4	11
619	A new family of urea-based low molecular-weight organogelators for environmental remediation: the influence of structure. Soft Matter, 2018, 14, 8821-8827.	2.7	11
620	Mitigation of hysteresis due to a pseudo-photochromic effect in thermochromic smart window coatings. Scientific Reports, 2018, 8, 13249.	3.3	11
621	Luminescence behaviour and deposition of Sc2O3 thin films from scandium(III) acetylacetonate at ambient pressure. Applied Physics Letters, 2018, 112, 221902.	3.3	11
622	Dual-scale TiO ₂ and SiO ₂ particles in combination with a fluoroalkylsilane and polydimethylsiloxane superhydrophobic/superoleophilic coating for efficient solvent–water separation. RSC Advances, 2019, 9, 20332-20340.	3.6	11
623	Cucurbituril-mediated quantum dot aggregates formed by aqueous self-assembly for sensing applications. Chemical Communications, 2019, 55, 5495-5498.	4.1	11
624	Ambipolar and Robust WSe 2 Fieldâ€Effect Transistors Utilizing Selfâ€Assembled Edge Oxides. Advanced Materials Interfaces, 2020, 7, 1901628.	3.7	11
625	Particle Size Evolution during the Synthesis of Gold Nanoparticles Using <i>In Situ</i> Time-Resolved UV–Vis Spectroscopy: An Experimental and Theoretical Study Unravelling the Effect of Adsorbed Gold Precursor Species. Journal of Physical Chemistry C, 2020, 124, 27662-27672.	3.1	11
626	Alkoxy derivatives of trithiazyltrichloride. Polyhedron, 1987, 6, 2161-2164.	2.2	10
627	Facile synthesis of SN and S–N–O complexes in liquid ammonia; X-ray structure of Pt[(HN)2SO2](PPh2Me)2. Journal of the Chemical Society Chemical Communications, 1989, , 1060-1061.	2.0	10
628	Mixed alkoxide-anilide d3-d3 dimers of molybdenum and tungsten. The X-ray crystal structures of M2(OBut)4(HNPh)2(H2NPh)2 (M = Mo, W). Polyhedron, 1991, 10, 2309-2316.	2.2	10
629	Homoleptic optically active ditungsten and dimolybdenum alkoxides. The crystal structure of (+)[W2(OC10H19)6]. Journal of the Chemical Society Dalton Transactions, 1992, , 2343.	1.1	10
630	Preparation of Fe–Zr–B amorphous alloys by chemical reduction. Journal of Materials Processing Technology, 1999, 92-93, 525-528.	6.3	10

#	Article	IF	CITATIONS
631	Platin-Komplexe der Anionen Se2N 22⊖ und Se2N2H⊖; Röntgenstrukturanalyse von [Pt(Se2N2H)(PMe2Ph)2]Cl. Angewandte Chemie, 2006, 101, 1052-1053.	2.0	10
632	Use of hydroxypropylmethylcellulose 2% for removing adherent silicone oil from silicone intraocular lenses. British Journal of Ophthalmology, 2009, 93, 1085-1088.	3.9	10
633	The reaction of tin(iv) iodide with phosphines: formation of new halotin anions. Dalton Transactions, 2009, , 10486.	3.3	10
634	Gas Sensing Properties of Composite Tungsten Trioxide-Zeolite Thick Films. ECS Transactions, 2009, 16, 77-84.	0.5	10
635	Atmospheric pressure chemical vapour deposition of NbSe2–TiSe2 composite thin films. Applied Surface Science, 2010, 256, 3178-3182.	6.1	10
636	Titanium arsenide films from the atmospheric pressure chemical vapour deposition of tetrakisdimethylamidotitanium and tert-butylarsine. Dalton Transactions, 2011, 40, 10664.	3.3	10
637	Thermal relaxation and collective dynamics of interacting aerosol-generated hexagonal NiFe2O4 nanoparticles. Physical Chemistry Chemical Physics, 2013, 15, 20830.	2.8	10
638	A Hierarchical MoO ₂ /Au/MnO ₂ HeteroÂstructure with Enhanced Electrochemical Performance for Application as Supercapacitor. European Journal of Inorganic Chemistry, 2015, 2015, 3764-3768.	2.0	10
639	A gas-sensing array produced from screen-printed, zeolite-modified chromium titanate. Measurement Science and Technology, 2015, 26, 085102.	2.6	10
640	Nanocellulose Derivative/Silica Hybrid Core-Shell Chiral Stationary Phase: Preparation and Enantioseparation Performance. Molecules, 2016, 21, 561.	3.8	10
641	Synthesis of Trimeric Organozinc Compounds and their Subsequent Reaction with Oxygen. ChemistryOpen, 2016, 5, 301-305.	1.9	10
642	Superhydrophobic Au/polymer nanocomposite films via AACVD/swell encapsulation tandem synthesis procedure. RSC Advances, 2016, 6, 31146-31152.	3.6	10
643	Si-doped zinc oxide transparent conducting oxides; nanoparticle optimisation, scale-up and thin film deposition. Journal of Materials Chemistry C, 2017, 5, 8796-8801.	5.5	10
644	Characterisation of VOCs Surrounding Naum Gabo's <i>Construction in Space †Two Cones</i> ', (Tate) by <i>in situ</i> SPME GC-MS Monitoring. Studies in Conservation, 2018, 63, 369-371.	1.1	10
645	Spacer-Defined Intrinsic Multiple Patterning. ACS Nano, 2020, 14, 12091-12100.	14.6	10
646	Liquid-microjet photoelectron spectroscopy of the green fluorescent protein chromophore. Nature Communications, 2022, 13, 507.	12.8	10
647	Robust superamphiphobic coatings with gradient and hierarchical architecture and excellent anti-flashover performances. Nano Research, 2022, 15, 7565-7576.	10.4	10
648	Triple bonds between molybdenum and tungsten atoms supported by selenolate ligands: M2(SeAr)6 and M2(OPri)2(SeAr)4(Ar = mesityl). Journal of the Chemical Society Chemical Communications, 1990, , 920.	2.0	9

#	Article	IF	CITATIONS
649	Preparation and characterisation of [Pt(SeSN2)(PR3)2], [Pt(Se2N2)(PR3)2], [Pt(SeSN2H)(PR3)2]BF4, and [Pt(Se2N2H)(PR3)2]BF4. Journal of the Chemical Society Dalton Transactions, 1990, , 925.	1.1	9
650	SELF PROPAGATING ROUTES TO GALLIUM AND INDIUM CHALCOGENIDES. Main Group Metal Chemistry, 1994, 17, .	1.6	9
651	Low-energy initiated routes to crystalline metal phosphides and arsenides. Journal of Materials Science Letters, 1994, 13, 1-2.	0.5	9
652	Atmospheric-Pressure CVD of Vanadium Oxynitride on Glass: Potential Solar Control Coatings. Chemical Vapor Deposition, 2000, 6, 59-63.	1.3	9
653	Dual-source chemical vapour deposition of titanium(III) phosphide from titanium tetrachloride and tristrimethylsilylphosphine. Applied Surface Science, 2003, 211, 2-5.	6.1	9
654	The use of hexamethyldisilathiane for the synthesis of transition metal sulfides. Polyhedron, 2003, 22, 1255-1262.	2.2	9
655	Synthesis and characterisation of tungsten(vi) oxo-salicylate complexes for use in the chemical vapour deposition of self-cleaning films. Dalton Transactions, 2005, , 1287.	3.3	9
656	Substrateâ€Dependant Ability of Titanium(IV) Oxide Photocatalytic Thin Films Prepared by Thermal CVD to Generate Hydrogen Gas from a Sacrificial Reaction. Chemical Vapor Deposition, 2010, 16, 301-304.	1.3	9
657	Impaired bacterial attachment to light activated Ni–Ti alloy. Materials Science and Engineering C, 2010, 30, 225-234.	7.3	9
658	Synthesis and Structural Characterization of βâ€Ketoiminate‣tabilized Gallium Hydrides for Chemical Vapor Deposition Applications. Chemistry - A European Journal, 2014, 20, 10503-10513.	3.3	9
659	Aerosol assisted chemical vapour deposition of transparent conductive aluminum-doped zinc oxide thin films from a zinc triflate precursor. Thin Solid Films, 2016, 616, 477-481.	1.8	9
660	Effects of bovine serum albumin on light activated antimicrobial surfaces. RSC Advances, 2018, 8, 34252-34258.	3.6	9
661	Effective onâ€line highâ€speed shear dispersing emulsifier technique coupled with highâ€performance countercurrent chromatography method for simultaneous extraction and isolation ofAcarotenoids from <i>Lycium barbarum</i> L. fruits. Journal of Separation Science, 2020, 43, 2949-2958.	2.5	9
662	Nonfluoride-modified halloysite nanotube-based hybrid: potential for acquiring super-hydrophobicity and improving flame retardancy of epoxy resin. Journal of Nanostructure in Chemistry, 2021, 11, 353-366.	9.1	9
663	Metathetical routes to uranium and thorium oxides and nitrides. Journal of Materials Science Letters, 1994, 13, 1185-1186.	0.5	8
664	Germanium phosphide coatings from the atmospheric pressure chemical vapour deposition of GeX4 (X=Cl or Br) and PCychexH2. Polyhedron, 2003, 22, 1683-1688.	2.2	8
665	Reactivity of tetrakisdimethylamido-titanium(iv) and -zirconium(iv) with thiols. New Journal of Chemistry, 2005, 29, 620.	2.8	8
666	Determination of the Optical Constants of VO ₂ and Nb-Doped VO ₂ Thin Films. Materials Science Forum, 0, 587-588, 640-644.	0.3	8

#	Article	IF	CITATIONS
667	Fabrication and characterization of Fe1.90Ti0.10O3 gas sensitive resistors for carbon monoxide. Sensors and Actuators B: Chemical, 2009, 135, 430-435.	7.8	8
668	High-Pressure Behavior and Polymorphism of Titanium Oxynitride Phase Ti _{2.85} O ₄ N. Journal of Physical Chemistry C, 2010, 114, 8546-8551.	3.1	8
669	Self-propagating high-temperature synthesis of aluminum substituted lanthanum ferrites LaFe _{1â^'x} Al _x O ₃ (0 ≤ ≤.0). New Journal of Chemistry, 2015, 39, 9834-9840.	2.8	8
670	Highly Photocatalytically Active Iron(III) Titanium Oxide Thin films via Aerosolâ€Assisted CVD. Chemical Vapor Deposition, 2015, 21, 21-25.	1.3	8
671	Ferrite Materials Produced From Self-Propagating High-Temperature Synthesis for Gas Sensing Applications. IEEE Sensors Journal, 2015, 15, 196-200.	4.7	8
672	Aerosol-assisted fabrication of tin-doped indium oxide ceramic thin films from nanoparticle suspensions. Journal of Materials Chemistry C, 2016, 4, 5739-5746.	5.5	8
673	Photobactericidal Activity of Dual Dyes Encapsulated in Silicone Enhanced by Silver Nanoparticles. ACS Omega, 2018, 3, 6779-6786.	3.5	8
674	A Hierarchical 3D TiO ₂ /Ni Nanostructure as an Efficient Holeâ€Extraction and Protection Layer for GaAs Photoanodes. ChemSusChem, 2020, 13, 6028-6036.	6.8	8
675	Probing the electronic and geometric structures of photoactive electrodeposited Cu2O films by X-ray absorption spectroscopy. Journal of Catalysis, 2020, 389, 483-491.	6.2	8
676	Thermoresponsive Black VO2–Carbon Nanotube Composite Coatings for Solar Energy Harvesting. ACS Applied Nano Materials, 2020, 3, 8848-8857.	5.0	8
677	Following the Formation of Silver Nanoparticles Using <i>In Situ</i> X-ray Absorption Spectroscopy. ACS Omega, 2020, 5, 13664-13671.	3.5	8
678	Zincâ€Ion Batteries: Multiâ€5cale Investigations of Î′â€Ni _{0.25} V ₂ O ₅ •nH ₂ O Cathode Materials in Aqueous Zincâ€Ion Batteries (Adv. Energy Mater. 15/2020). Advanced Energy Materials, 2020, 10, 2070068.	19.5	8
679	Strong robust superhydrophobic C/silicone monolith for photothermal ice removal. Journal of Materials Science, 2022, 57, 6963-6970.	3.7	8
680	Room Temperature Synthesis in Liquid Ammonia of Zinc, Cadmium, and Mercury Sulfides. Main Group Chemistry, 1996, 1, 183-187.	0.8	7
681	Synthesis and Charaterisation of Chromium Oxyselenide (Cr2Se0.7O2.3) Formed from Chemical Vapour Synthesis: A New Antiferromagnet. European Journal of Inorganic Chemistry, 2007, 2007, 4579-4582.	2.0	7
682	A Highly Effective Pt and H3PW12O40 Modified Zirconium Oxide Metal–Acid Bifunctional Catalyst for Skeletal Isomerization: Preparation, Characterization and Catalytic Behavior Study. Catalysis Letters, 2008, 125, 340-347.	2.6	7
683	Combinatorial CVD: New Oxynitride Photocatalysts. ECS Transactions, 2009, 25, 139-154.	0.5	7
684	Combinatorial CVD: New Oxy-nitride Photocatalysts. ECS Transactions, 2009, 25, 1239-1250.	0.5	7

#	Article	IF	CITATIONS
685	Gas-sensing properties of Fe2â^xTixO3+γ (x=0–1.4). Polyhedron, 2010, 29, 1225-1230.	2.2	7
686	Single-step synthesis of doped TiO2 stratified thin-films by atmospheric-pressure chemical vapour deposition. Journal of Materials Chemistry A, 2014, 2, 7082.	10.3	7
687	Polyoxometalate Complexes as Precursors to Vanadiumâ€Doped Molybdenum or Tungsten Oxide Thin Films by Means of Aerosolâ€Assisted Chemical Vapour Deposition. ChemPlusChem, 2016, 81, 307-314.	2.8	7
688	Battery Electrodes: A Dendritic Nickel Cobalt Sulfide Nanostructure for Alkaline Battery Electrodes (Adv. Funct. Mater. 23/2018). Advanced Functional Materials, 2018, 28, 1870154.	14.9	7
689	Continuous Single-Phase Synthesis of [Au25(Cys)18] Nanoclusters and their Photobactericidal Enhancement. ACS Applied Materials & Interfaces, 2020, 12, 49021-49029.	8.0	7
690	Probing Mg Intercalation in the Tetragonal Tungsten Bronze Framework V ₄ Nb ₁₈ O ₅₅ . Inorganic Chemistry, 2020, 59, 9783-9797.	4.0	7
691	A route to engineered high aspect-ratio silicon nanostructures through regenerative secondary mask lithography. Nanoscale, 2022, 14, 1847-1854.	5.6	7
692	Mussel-Inspired Interfacial Modification for Ultra-Stable MoS ₂ Lubricating Films with Improved Tribological Behavior on Nano-Textured ZnO Surfaces Using the AACVD Method. ACS Applied Materials & Interfaces, 2022, 14, 27484-27494.	8.0	7
693	Coupling constants incis-phosphine platinum complexes containing chalcogen-nitride anions. Heteroatom Chemistry, 1991, 2, 301-305.	0.7	6
694	Enhancement by Nanogold of the Efficacy of a Light-Activated Antimicrobial Coating. Current Nanoscience, 2009, 5, 257-261.	1.2	6
695	Improved Texturing and Photocatalytic Efficiency in Ti <scp>O</scp> ₂ Films Grown Using Aerosolâ€ <scp>A</scp> ssisted <scp>CVD</scp> and Atmospheric Pressure CVD. Chemical Vapor Deposition, 2013, 19, 355-362.	1.3	6
696	High-throughput synthesis of core–shell and multi-shelled materials by fluidised bed chemical vapour deposition. Case study: double-shell rutile–anatase particles. Journal of Materials Chemistry A, 2015, 3, 17241-17247.	10.3	6
697	In situ mass spectrometry analysis of chemical vapour deposition of TiO ₂ thin films to study gas phase mechanisms. RSC Advances, 2016, 6, 111797-111805.	3.6	6
698	[{VOCl2(CH2(COOEt)2)}4] as a molecular precursor for thermochromic monoclinic VO2 thin films and nanoparticles. Journal of Materials Chemistry C, 2016, 4, 10453-10463.	5.5	6
699	Zeolite Modified Vanadium Pentoxide Sensors for the Selective Detection of Volatile Organic Compounds. MRS Advances, 2016, 1, 3349-3354.	0.9	6
700	Switchable changes in the conductance of single-walled carbon nanotube networks on exposure to water vapour. Nanoscale, 2017, 9, 11279-11287.	5.6	6
701	Reflective Silver Thin Film Electrodes from Commercial Silver(I) Triflate via Aerosol-Assisted Chemical Vapor Deposition. ACS Applied Nano Materials, 2018, 1, 3724-3732.	5.0	6
702	Oneâ€step synthesis of Ag@PS nanospheres via flash nanoprecipitation. Applied Organometallic Chemistry, 2019, 33, e4713.	3.5	6

#	Article	IF	CITATIONS
703	Cocaine by-product detection with metal oxide semiconductor sensor arrays. RSC Advances, 2020, 10, 28464-28477.	3.6	6
704	Synergistic interactions of cadmium-free quantum dots embedded in a photosensitised polymer surface: efficient killing of multidrug-resistant strains at low ambient light levels. Nanoscale, 2020, 12, 10609-10622.	5.6	6
705	The effect of Cu dopants on electron transfer to O ₂ and the connection with acetone photocatalytic oxidations over nano-TiO ₂ . Physical Chemistry Chemical Physics, 2021, 23, 8300-8308.	2.8	6
706	The preparation and X-ray structure of Pt(PMe2Ph)2[S2N3(SO2)(NH2)]. Journal of the Chemical Society Chemical Communications, 1989, , 58.	2.0	5
707	A convenient, rapid, low-energy route to crystalline TIN, VN and Ti x V y N (x + y = 1). Journal of Materials Science Letters, 1993, 12, 1856-1857.	0.5	5
708	Solid state metathesis preparations of group VIII metal oxide powders. Journal of Materials Science Letters, 1994, 13, 219-221.	0.5	5
709	Self propagating high temperature synthesis of BaTiO3 using titanium trichloride as a fuel source. Journal of Materials Science Letters, 1996, 15, 542-543.	0.5	5
710	Novel SHS routes to CoTi-doped M-type ferrites. Journal of Materials Science: Materials in Electronics, 2001, 12, 533-536.	2.2	5
711	N-doped Titania Thin Films, Prepared by Atmospheric Pressure Chemical Vapour Deposition: Enhanced Visible Light Photocatalytic Activity and Anti-microbial Effects. ECS Transactions, 2009, 25, 65-72.	0.5	5
712	Enhanced Solubility and Covalent Functionalisation of Single Walled Carbon Nanotubes via Atmospheric Pressure Microwave Reflux and the Subsequent Spray Coating of Transparent Conducting Thin Films. Current Nanoscience, 2010, 6, 232-242.	1.2	5
713	Novel ion pairs obtained from the reaction of titanium(IV) halides with simple arsane ligands. Acta Crystallographica Section C: Crystal Structure Communications, 2011, 67, m96-m99.	0.4	5
714	Zeolite films: a new synthetic approach. Journal of Materials Chemistry A, 2013, 1, 1388-1393.	10.3	5
715	Gas sensing studies of an n-n heterojunction metal oxide semiconductor sensor array based on WO <inf>3</inf> and ZnO composites. , 2013, , .		5
716	Chromatographic Evaluation of Octadecyl-Bonded SiO2/SiO2-Based Stationary Phase for Reversed-Phase High Performance Liquid Chromatography. Journal of Inorganic and Organometallic Polymers and Materials, 2013, 23, 1445-1450.	3.7	5
717	The use of time resolved aerosol assisted chemical vapour deposition in mapping metal oxide thin film growth and fine tuning functional properties. Journal of Materials Chemistry A, 2015, 3, 4811-4819.	10.3	5
718	Ethanol sensing characteristics of Zn _{0.99} M _{0.01} O (M = Al/Ni) nanopowders. Physica Status Solidi (A) Applications and Materials Science, 2016, 213, 203-209.	1.8	5
719	The Effect of Alkali Metal (Na, K) Doping on Thermochromic Properties of VO2 Films. MRS Advances, 2018, 3, 1863-1869.	0.9	5
720	Influence of Lithium and Lanthanum Treatment on TiO 2 Nanofibers and Their Application in nâ€iâ€p Solar Cells. ChemElectroChem, 2019, 6, 3590-3598.	3.4	5

#	Article	IF	CITATIONS
721	Qualitative Approaches Towards Useful Photocatalytic Materials. Frontiers in Chemistry, 2020, 8, 817.	3.6	5
722	Some peculiarities of room-temperature ferromagnetism in ensembles of mixed-phase TiNx-TiOy nanoparticles. Materials Research Bulletin, 2021, 134, 111092.	5.2	5
723	Multifunctional two-dimensional glassy graphene devices for vis-NIR photodetection and volatile organic compound sensing. Science China Materials, 2021, 64, 1964-1976.	6.3	5
724	Zincâ€lon Batteries: Insights on Flexible Zincâ€lon Batteries from Lab Research to Commercialization (Adv.) Tj ET	Qq0001	gBŢ /Overloo
725	Synthesis of superhydrophobic polymer/tungsten (VI) oxide nanocomposite thin films. European Journal of Chemistry, 2016, 7, 139-145.	0.6	5
726	Fabrication of C-Doped Titanium Dioxide Coatings with Improved Anti-icing and Tribological Behavior. Langmuir, 2022, 38, 576-583.	3.5	5
797	Synthesis and structural characterisation of titanium(IV) thiolate compounds. Dalton Transactions	23	4

727	RSC, 2000, , 3500-3504.	2.3	4
728	Intelligent Window Coatings: Atmospheric Pressure Chemical Vapor Deposition of Tungsten-Doped Vanadium Dioxide ChemInform, 2004, 35, no.	0.0	4
729	Phase composition and magnetism of combustion products in Ba–Fe–O compounds synthesized under applied DC electric field. Journal of Magnetism and Magnetic Materials, 2007, 309, 202-206.	2.3	4
730	Zeolite-based discriminating gas sensors. Studies in Surface Science and Catalysis, 2008, 174, 549-554.	1.5	4
731	Zeolite Modification: Towards Discriminating Metal Oxide Gas Sensors. ECS Transactions, 2009, 19, 241-250.	0.5	4
732	Electromotive force measurements in the combustion wave front during layer-by-layer surface laser sintering of exothermic powder compositions. Physical Chemistry Chemical Physics, 2009, 11, 3503.	2.8	4
733	Aerosol Assisted Depositions of Polymers Using an Atomiser Delivery System. Journal of Nanoscience and Nanotechnology, 2011, 11, 8358-8362.	0.9	4
734	Special Section on the CVD of TiO2 and Doped TiO2 Films. Chemical Vapor Deposition, 2012, 18, 87-88.	1.3	4
735	Magnesium Oxide Thin Films with Tunable Crystallographic Preferred Orientation via Aerosolâ€Assisted CVD. Chemical Vapor Deposition, 2015, 21, 145-149.	1.3	4
736	Antimicrobial Surfaces: Dualâ€Mechanism Antimicrobial Polymer–ZnO Nanoparticle and Crystal Violetâ€Encapsulated Silicone (Adv. Funct. Mater. 9/2015). Advanced Functional Materials, 2015, 25, 1366-1366.	14.9	4
737	Controlling and modelling the wetting properties of III-V semiconductor surfaces using re-entrant nanostructures. Scientific Reports, 2018, 8, 3544.	3.3	4

738Tuning operating temperature of BaSnO3 gas sensor for reducing and oxidizing gases. AIP Conference
Proceedings, 2018, , .0.44

#	Article	IF	CITATIONS
739	Macroscale Superlubricity: Macroscale Superlubricity Enabled by Grapheneâ€Coated Surfaces (Adv. Sci.) Tj ETQq1	10,7843 11.2	14 rgBT /O
740	Assessment of GaPSb/Si tandem material association properties for photoelectrochemical cells. Solar Energy Materials and Solar Cells, 2021, 221, 110888.	6.2	4
741	A light–heat synergism in the sub-bandgap photocatalytic response of pristine TiO ₂ : a study of <i>in situ</i> diffusion reflectance and conductance. Physical Chemistry Chemical Physics, 2022, 24, 5618-5626.	2.8	4
742	Mo/Fe bimetallic pyrophosphates derived from Prussian blue analogues for rapid electrocatalytic oxygen evolution. Green Energy and Environment, 2023, 8, 1450-1458.	8.7	4
743	Synthesis and properties of bis-imido complexes of the type Pt(NH)2C6H3NO2(PR3)2 from reactions in liquid ammonia. X-ray structure of Pt(NH)2C6H3NO2(PMePh2)2. Polyhedron, 1989, 8, 2507-2511.	2.2	3
744	DESIGNING PRECURSORS FOR THE DEPOSITION OF TIN SULPHIDE THIN FILMS. Main Group Metal Chemistry, 2001, 24, .	1.6	3
745	Hybrid Aerosol Assisted Atmospheric Pressure Chemical Vapour Deposition: A Facile Route Toward Nano-Composite Thin Films?. ECS Transactions, 2009, 25, 773-780.	0.5	3
746	The Support Effect over Pt–H3PW12O40 Based Metal-Acid Bifunctional Catalysts on the Catalytic Performance in n-Pentane Isomerization. Catalysis Letters, 2009, 129, 215-221.	2.6	3
747	Evaluating Zeolite-Modified Sensors: towards a faster set of chemical sensors. , 2011, , .		3
748	Titania Coated Mica via Chemical Vapour Deposition, Post N-doped by Liquid Ammonia Treatment. Physics Procedia, 2013, 46, 111-117.	1.2	3
749	Mesenchymal stem cell response to UV-photofunctionalized TiO ₂ coated CoCrMo. RSC Advances, 2014, 4, 59847-59857.	3.6	3
750	Silicalite-1/glass fibre substrates for enhancing the photocatalytic activity of TiO2. RSC Advances, 2015, 5, 6970-6975.	3.6	3
751	Light-driven generation of chlorine and hydrogen from brine using highly selective Ru/Ti oxide redox catalysts. Sustainable Energy and Fuels, 2017, 1, 254-257.	4.9	3
752	A Comparison of the Potential Capability of SFS, SPS and HVSFS for the Production of Photocatalytic Titania Coatings. Journal of Thermal Spray Technology, 2017, 26, 161-172.	3.1	3
753	Carboxylic Acid Functionalization at the Meso-Position of the Bodipy Core and Its Influence on Photovoltaic Performance. Nanomaterials, 2019, 9, 1346.	4.1	3
754	Surface Oxygen Vacancies: Dynamics of Photoâ€Induced Surface Oxygen Vacancies in Metalâ€Oxide Semiconductors Studied Under Ambient Conditions (Adv. Sci. 22/2019). Advanced Science, 2019, 6, 1970132.	11.2	3
755	Self-healing on mismatched fractured composite surfaces of SiC with a diameter of 180 nm. Nanoscale, 2020, 12, 19617-19627.	5.6	3
756	A combined experimental and theoretical study into the performance of multilayer vanadium dioxide		3

nanocomposites for energy saving applications. , 2018, , .

#	Article	IF	CITATIONS
757	Ultra high molecular weight polyethylene with incorporated crystal violet and gold nanoclusters is antimicrobial in low intensity light and in the dark. Materials Advances, 2020, 1, 3339-3348.	5.4	3
758	Facile formation of black titania films using an atmospheric-pressure plasma jet. Green Chemistry, 2022, 24, 2499-2505.	9.0	3
759	NEW SYNTHETIC ROUTES TO S ₄ N ₄ and S ₇ NH. REACTION OF Li ₃ N WITH S ₃ N ₃ Cl ₃ AND SCl ₂ . Phosphorus, Sulfur and Silicon and the Related Elements, 1990, 47, 141-143.	1.6	2
760	Preparation of FeMnB Alloys by Chemical Reduction. Journal of Materials Science Letters, 1999, 18, 39-40.	0.5	2
761	Combustion synthesis of sodium-substituted lanthanum manganites. Mendeleev Communications, 2006, 16, 36-38.	1.6	2
762	SHS in the UK: Past, present, and future directions. International Journal of Self-Propagating High-Temperature Synthesis, 2008, 17, 266-274.	0.5	2
763	Control of ZnO Nanostructures via Vapor Transport. Chemical Vapor Deposition, 2012, 18, 282-288.	1.3	2
764	A neutron diffraction study of oxygen and nitrogen ordering in a kinetically stable orthorhombic iron doped titanium oxynitride. Journal of Solid State Chemistry, 2012, 190, 169-173.	2.9	2
765	Atmospheric pressure chemical vapour deposition of vanadium arsenide thin films via the reaction of VCl4 or VOCl3 with tBuAsH2. Thin Solid Films, 2013, 537, 171-175.	1.8	2
766	Ferrite materials for gas sensing applications. , 2013, , .		2
767	Oil Spills: Barrel-Shaped Oil Skimmer Designed for Collection of Oil from Spills (Adv. Mater.) Tj ETQq1 1 0.7843	14 rgBT /O	verlock 10 Tf
768	Synthesis and Characterisation of Various Diester and Triester Adducts of TiCl ₄ . European Journal of Inorganic Chemistry, 2015, 2015, 3666-3673.	2.0	2
769	Electrochemical Properties of APCVD αâ€Fe ₂ O ₃ Nanoparticles at 300 ^o C. ChemistrySelect, 2016, 1, 2228-2234.	1.5	2
770	Enhancing the Magnetic Heating Capacity of Iron Oxide Nanoparticles through Their Postproduction Incorporation into Iron Oxide-Gold Nanocomposites. European Journal of Inorganic Chemistry, 2017, 2017, 2385-2385.	2.0	2
771	{Ni4O4} Cluster Complex to Enhance the Reductive Photocurrent Response on Silicon Nanowire Photocathodes. Nanomaterials, 2017, 7, 33.	4.1	2
772	Charge carrier transfer in photocatalysis. Interface Science and Technology, 2020, , 103-159.	3.3	2
773	Modelling and measurement of laser-generated focused ultrasound: Can interventional transducers achieve therapeutic effects?. Journal of the Acoustical Society of America, 2021, 149, 2732-2742.	1.1	2
774	High Surface Area of Polyhedral Chromia and Hexagonal Chromium Sulfide by the Thermolysis of Cyclohexylammonium Hexaisothiocyanatochromate(III) Sesquihydrate. ChemistrySelect, 2021, 6, 4298-4311.	1.5	2

#	Article	IF	CITATIONS
775	Photo-induced enhanced Raman spectroscopy (PIERS): sensing atomic-defects, explosives and biomolecules. , 2019, , .		2
776	Universal Theory of Light Scattering of Randomly Oriented Particles: A Fluctuational-Electrodynamics Approach for Light Transport Modeling in Disordered Nanostructures. ACS Photonics, 2022, 9, 672-681.	6.6	2
777	Exchange-Driven Magnetic Anomalies in Fe–Zr–B-Based Nanocomposites. Hyperfine Interactions, 2002, 144/145, 223-230.	0.5	1
778	Synthesis and properties of nickel–cobalt–boron nanoparticles. Journal of Physics: Conference Series, 2005, 17, 196-200.	0.4	1
779	Particle Size and Oxidation in CoNi Nanoparticles. Materials Research Society Symposia Proceedings, 2005, 877, 1.	0.1	1
780	Discrimination effects in zeolite modified metal oxide semiconductor gas sensors. , 2009, , .		1
781	Optimisation of Thermochromic Thin Films on Glass; Design of Intelligent Windows. Advances in Science and Technology, 0, , .	0.2	1
782	The influence of a dc electric field on chemical interactions in "peroxide-metal―systems during combustion processes. New Journal of Chemistry, 2010, 34, 391.	2.8	1
783	Oxide Nanoparticle Thin Films Created Using Molecular Templates. Journal of Physical Chemistry C, 2011, 115, 13151-13157.	3.1	1
784	Di-μ-chlorido-bis[dichloridobis(methylamido-κN)bis(methylamine-κN)titanium(IV)]. Acta Crystallographica Section C: Crystal Structure Communications, 2011, 67, m234-m236.	0.4	1
785	Synthesis of Rutile Nb:TiO ₂ Freeâ€Standing Thin Film at the Liquid–Air Interface. Advanced Materials Interfaces, 2016, 3, 1600361.	3.7	1
786	Advanced Compositional Analysis of Nanoparticle-polymer Composites Using Direct Fluorescence Imaging. Journal of Visualized Experiments, 2016, , .	0.3	1
787	Photocatalysis: Evidence and Effect of Photogenerated Charge Transfer for Enhanced Photocatalysis in WO ₃ /TiO ₂ Heterojunction Films: A Computational and Experimental Study (Adv. Funct. Mater. 18/2017). Advanced Functional Materials, 2017, 27, .	14.9	1
788	Dopant stability in multifunctional doped TiO ₂ 's under environmental UVA exposure. Environmental Science: Nano, 2017, 4, 1108-1113.	4.3	1
789	57Fe Mössbauer study of NiFe2O4 nanoparticles produced by the levitation-jet aerosol technique. Journal of Materials Science: Materials in Electronics, 2018, 29, 14347-14352.	2.2	1
790	Multivalent Ion Batteries: Cathode Design for Aqueous Rechargeable Multivalent Ion Batteries: Challenges and Opportunities (Adv. Funct. Mater. 13/2021). Advanced Functional Materials, 2021, 31, 2170089.	14.9	1
791	Flame retardant and superhydrophobic composites via oriented arrangement of boron nitride nanosheets. Journal of Materials Science, 2021, 56, 19955-19968.	3.7	1
792	A study of the interaction of cationic dyes with gold nanostructures. RSC Advances, 2021, 11, 17694-17703.	3.6	1

#	Article	IF	CITATIONS
793	Rapid, Solid-State Metathesis Routes to Metal Carbides. , 1998, 10, 805.		1
794	Rapid, Solid-State Metathesis Routes to Metal Carbides. Advanced Materials, 1998, 10, 805-808.	21.0	1
795	The Gas Sensing Properties of Zinc Stannates Prepared by Self-Propagating High-Temperature Synthesis. Sensor Letters, 2014, 12, 1567-1571.	0.4	1
796	Quantitative SERS Detection of Uric Acid via Formation of Precise Plasmonic Nanojunctions within Aggregates of Gold Nanoparticles and Cucurbit[n]uril. Journal of Visualized Experiments, 2020, , .	0.3	1
797	Metalla-Sulphur-Nitrogen Chemistry. Phosphorus, Sulfur and Silicon and the Related Elements, 1989, 41, 223-228.	1.6	0
798	A convenient route to crystalline LiLnS2 (Ln = Nd, Sm, Gd, Tb, Dy, Ho, Er, Yb) and Ln x ,S y (Ln = La, Ce,) Tj ETQqC	0 0 0 rgBT	/Overlock 10
799	Synthesis of Amorphous Fe-Zr-B by Chemical Reduction. Journal of Materials Science Letters, 1999, 18, 425-426.	0.5	0
800	Chemical Reactions in Applied Magnetic Fields. , 0, , 467-481.		0
801	Anatase Thin Films on Glass from the Chemical Vapor Deposition of Titanium(IV) Chloride and Ethyl Acetate ChemInform, 2003, 34, no.	0.0	0
802	Solvent-Free Reactions in the Solid State: Solid State Metathesis. ChemInform, 2003, 34, no.	0.0	0
803	Electrochemistry and Dynamic Ionography of Self-Propagating High-Temperature Synthesis (SHS). Materials Science Forum, 2007, 555, 73-81.	0.3	0
804	Chapter 10. CVD of Functional Coatings on Glass. , 0, , 451-476.		0
805	The Synthesis of Tantalum (V) Oxide Using Atmospheric Pressure Chemical Vapour Deposition for the Purposes of Photo-activated Water Splitting. ECS Transactions, 2009, 25, 935-942.	0.5	0
806	Zeolite Modified Discriminating Gas Sensors. ECS Transactions, 2008, 16, 275-286.	0.5	0
807	A Single-Step Route Towards Large-Scale Deposition of Nanocomposite Thin Films Using Preformed Gold Nanoparticles. Materials Research Society Symposia Proceedings, 2009, 1174, 13.	0.1	0
808	Features of power engineering in a dynamic electrically conductive medium. International Journal of Self-Propagating High-Temperature Synthesis, 2009, 18, 76-86.	0.5	0
809	One-Step Synthesis of CuO Films Composed of Three-Dimensional Microflowers on Copper Surfaces. Journal of Nanoscience and Nanotechnology, 2009, 9, 1568-1570.	0.9	0
810	SHS of metal-oxide systems in a DC magnetic field: Part 1. TRXRD and thermal imaging studies of the Fe-Fe2O3 system. International Journal of Self-Propagating High-Temperature Synthesis, 2011, 20, 40-47.	0.5	0

#	Article	IF	CITATIONS
811	SHS of transition metal-oxide systems in a DC magnetic field: Part 2. TRXRD, thermal imaging, and chemomagnetic studies of metal-oxide systems. International Journal of Self-Propagating High-Temperature Synthesis, 2011, 20, 48-52.	0.5	0
812	Influence of Lithium and Lanthanum Treatment on TiO 2 Nanofibers and Their Application in nâ€iâ€p Solar Cells. ChemElectroChem, 2019, 6, 3529-3529.	3.4	0
813	Influence of Humidity on the NO2 Sensing Properties of SrCo0.1Ti0.9O3. Springer Proceedings in Physics, 2019, , 905-911.	0.2	0
814	Generating, probing and utilising photo-induced surface oxygen vacancies for trace molecular detection. , 2021, , .		0
815	CuInS ₂ Quantum Dot and Polydimethylsiloxane Nanocomposites for Allâ€Optical Ultrasound and Photoacoustic Imaging (Adv. Mater. Interfaces 20/2021). Advanced Materials Interfaces, 2021, 8, 2170114.	3.7	0
816	Optical fiber laser ultrasound transmitter with electrospun composite for minimally invasive medical imaging. , 2017, , .		0
817	Adsorptivity of Some Organic Compounds to Copper Nanoparticles. International Journal of Self-Propagating High-Temperature Synthesis, 2022, 31, 47-50.	0.5	0
818	Hydrogenation of Xylenes, Ethylbenzene, and Isopropylbenzene on Ni Nanoparticles. International Journal of Self-Propagating High-Temperature Synthesis, 2022, 31, 42-46.	0.5	0